

The dark matter transfer function: free streaming, particle statistics and memory of gravitational clustering.

D. Boyanovsky^{(a,b,c),*} H. J. de Vega^{(b,c),†} and N. G. Sanchez^{(c)‡}

^(a) Department of Physics and Astronomy, University of Pittsburgh, Pittsburgh, Pennsylvania 15260, USA.

^(b) LPTHE, Laboratoire Associé au CNRS UMR 7589,

Université Pierre et Marie Curie (Paris VI) et Denis Diderot (Paris VII),
Tour 24, 5^{ème}. étage, 4, Place Jussieu, 75252 Paris, Cedex 05, France.

^(c) Observatoire de Paris, LERMA, Laboratoire Associé au CNRS UMR 8112,
61, Avenue de l'Observatoire, 75014 Paris, France.

(Dated: October 25, 2018)

The transfer function $T(k)$ of dark matter (DM) perturbations during matter domination is obtained by solving the linearized collisionless Boltzmann-Vlasov equation. We provide an *exact* expression for $T(k)$ for *arbitrary distribution functions of decoupled particles and initial conditions*, which can be systematically expanded in a Fredholm series. An exhaustive numerical study of thermal relics for different initial conditions reveals that the first *two* terms in the expansion of $T(k)$ provide a remarkably accurate and simple approximation valid on all scales of cosmological relevance for structure formation in the linear regime. The natural scale of suppression is the free streaming wavevector at matter-radiation equality, $k_{fs}(t_{eq}) = \left[4\pi\rho_{0M}/[(\bar{V}^2)(1+z_{eq})]\right]^{\frac{1}{2}}$. An important ingredient is a non-local kernel determined by the distribution functions of the decoupled particles which describes the *memory of the initial conditions and gravitational clustering* and yields a correction to the fluid description. This correction is negligible at large scales $k \ll k_{fs}(t_{eq})$ but it becomes important at small scales $k \geq k_{fs}(t_{eq})$. Distribution functions that favor the small momentum region yield longer-range memory kernels and lead to an *enhancement of power at small scales* $k > k_{fs}(t_{eq})$. Fermi-Dirac and Bose-Einstein statistics lead to long-range memory kernels, with longer range for bosons, both resulting in enhancement of $T(k)$ at small scales. For DM thermal relics that decoupled while ultrarelativistic we find $k_{fs}(t_{eq}) \simeq 0.003 (g_d/2)^{\frac{1}{3}} (m/\text{keV}) [\text{kpc}]^{-1}$, where g_d is the number of degrees of freedom at decoupling. For WIMPS we obtain $k_{fs}(t_{eq}) = 5.88 (g_d/2)^{\frac{1}{3}} (m/100 \text{ GeV})^{\frac{1}{2}} (T_d/10 \text{ MeV})^{\frac{1}{2}} [\text{pc}]^{-1}$. For $k \ll k_{fs}(t_{eq})$, $T(k) \sim 1 - C[k/k_{fs}(t_{eq})]^2$ where $C = \mathcal{O}(1)$ and independent of statistics for thermal relics. We provide simple and accurate fits for $T(k)$ in a wide range of *small* scales $k > k_{fs}(t_{eq})$ for thermal relics and different initial conditions. The numerical and analytic results for *arbitrary* distribution functions and initial conditions allow an assessment of DM candidates through their impact on structure formation.

Contents

I. Introduction and Results	2
II. Gilbert's Equation	5
A. The free streaming length.	7
B. Exact results from Gilbert's equation	10
C. Thermal and Gilbert's initial conditions	11
D. Solution of the Gilbert equation in powers of k .	12
E. Gilbert's equation as an integro-differential equation.	12
F. The <i>exact</i> transfer function and its Fredholm expansion.	14
III. Cold Dark Matter: Non-relativistic, Maxwell-Boltzmann distribution.	17
A. Short wavelength: memory of gravitational clustering	19
IV. Warm and hot dark matter: Fermions vs. Bosons	22
A. Fermions	23

*Electronic address: boyan@pitt.edu

†Electronic address: devega@lpthe.jussieu.fr

‡Electronic address: Norma.Sanchez@obspm.fr

B. Bosons	25
V. Small scales: statistics and memory of gravitational clustering	27
VI. Conclusions	30
Acknowledgments	32
References	32

I. INTRODUCTION AND RESULTS

The *concordance* Λ CDM standard cosmological model successfully explains a wide range of highly precise astrophysical and cosmological observations. Main ingredients are an early stage of accelerated expansion (inflation) a more recent stage of accelerated expansion driven by dark energy, and the presence of dark matter (DM) composed of primordial particles which are cold and collisionless at the time when the first structures formed [1, 2].

In the cold dark matter (CDM) model, structure formation proceeds in a hierarchical bottom up approach: small scales become non-linear and collapse first and their merger and accretion leads to structure on larger scales. This is a consequence of the fact that CDM features negligible small velocity dispersions leading to a power spectrum that favors small scales. In this hierarchical scenario, dense clumps that survive the merger process form satellite galaxies.

Large scale Λ CDM simulations seemingly lead to an overprediction of satellite galaxies [3] by almost an order of magnitude over the number of satellites that have been observed in Milky-Way sized galaxies [3, 4, 5, 6, 7]. These simulations also yield a distinct prediction: virialized DM halos should feature a density profile that increases monotonically towards the center [3, 8, 9, 10, 11] such as the Navarro-Frenk-White (NFW) profile [8] or more general central density profiles $\rho(r) \sim r^{-\beta}$ with $1 \leq \beta \lesssim 1.5$ [5, 8, 11]. These profiles accurately describe clusters of galaxies but indicate a divergent cusp at the center of the halo.

There is, however, an accumulating body of observational evidence [12, 13, 14, 15, 16, 17, 18, 19] that seem to indicate that the density profile in the central regions of dwarf galaxies is smooth leading to the suggestion that the central regions feature smooth cores instead of cusps as predicted by CDM.

Warm dark matter (WDM) particles were invoked [20, 21, 22] as possible solutions to the above mentioned discrepancies both in the overabundance of satellite galaxies and as a mechanism to smooth out the cusped density profiles predicted by CDM simulations into the cored profiles seemingly observed in dwarf-spheroidal satellite galaxies (dSphs). WDM particles feature a range of velocity dispersion in between the CDM and hot dark matter (HDM) leading to free streaming scales that smoothes out small scale features and could be consistent with core radii of the dSphs.

Even if these problems of the CDM model find other astrophysical solutions, it remains an important and intrinsically interesting question to assess the clustering properties of WDM candidates, since these may emerge from extensions beyond the standard model of particle physics. Furthermore, it remains an important aspect to understand possible departures of the CDM paradigm at small scales provided by alternative particle physics candidates.

The gravitational clustering properties of collisionless DM in the linear regime are described by the power spectrum of gravitational perturbations and in particular the transfer function that converts the primordial power spectrum into the power spectrum later in the matter dominated era, which in turn, is the input in the large scale numerical simulations of galaxy formation. Free streaming [2] of collisionless DM leads to a suppression of the transfer function on length scales smaller than the free streaming scale via Landau damping [23].

Perturbations in a collisionless system of particles with gravitational interactions is fundamentally different from fluid perturbations in the presence of gravity. The (perfect) fluid equations correspond to the limit of vanishing mean free path. In a gravitating fluid, pressure gradients tend to restore hydrostatic equilibrium with the speed of sound in the medium, and short wavelength fluctuations are simple acoustic waves. For large wavelengths, the propagation of pressure waves cannot halt gravitational collapse on a dynamical time scale. The dividing line is the Jeans length: perturbations with shorter wavelengths oscillate as sound waves, while perturbations with longer wavelengths undergo gravitational collapse.

In a gas of collisionless particles with gravitational interaction the situation is different since the mean free path is much larger than the size of the system (Hubble radius) and the fluid description is not valid. Instead, the collisionless Boltzmann-Vlasov equation for the distribution function must be solved to obtain the dynamics of perturbations [1, 24, 25].

Just as in the case of plasma physics, the linearized Boltzmann-Vlasov equation describes *collective* excitations [26]. In the case of a collisionless gas with gravitational interactions these collective excitations describe particles free-streaming in and out of the gravitational potential wells of which they are the source. The damping of short wavelength *collective* excitations is akin to *Landau damping in plasmas* [26]: it is a result of *dephasing* via phase mixing when the particles are out of phase with the potential wells that they produce [27] and leads to the collisionless damping of the collective modes [28].

Gilbert [29] studied the linearized Boltzmann-Vlasov equation in a matter dominated cosmology for non-relativistic particles described by an (unperturbed) Maxwell-Boltzmann distribution function. This equation was cast as a Volterra integral equation whose numerical solution revealed a limiting value of the wavevector above which density perturbations are Landau damped and below which they grow via gravitational (Jeans) instability [29]. The results were consistent with replacing the speed of sound by the Maxwellian velocity dispersion in the Jeans length [up to a normalization factor of $\mathcal{O}(1)$]. Gilbert's equations were solved numerically to study: (i) the collisionless damping of density fluctuations in an expanding cosmology with massive neutrinos with an approximated Fermi-Dirac distribution function [23]; (ii) the dissipationless clustering of neutrinos with a truncation of the Fermi-Dirac distribution function and an analytic fit to the numerical solution of the integral equation [30]. These results were also used to analyze the linear regime [21]; (iii) cosmological perturbations and massive light neutrinos [25, 31], and more recently similar integral equations were solved approximately for thermal neutrino relics [32].

DM may be composed of several species [33], a possibility that can be accommodated in most extensions of the Standard Model, with candidates ranging from weakly interacting massive particles (WIMPs) [2] to axions [2] and sterile neutrinos [34, 35, 36]. DM candidates may be produced in the early Universe via different mechanisms and some of them are conjectured to decouple and freeze-out with non-thermal distribution functions. Sterile neutrinos are an example of this DM candidate [34, 35, 36]. It is important to understand the clustering properties of possible DM particles that decoupled *in or out* of local thermal equilibrium. Predictions for the effective free-streaming length and transfer function are a necessary ingredient in the study of structure formation. The free-streaming length in such *mixture* was recently investigated in ref. [37] for *arbitrary* distribution functions of relic particles that decoupled in or out local thermodynamic equilibrium (LTE). This study analyzed the Boltzmann-Vlasov equation in Minkowski space-time focusing on the marginally unstable collective modes. It revealed important (and intriguing) aspects of the free streaming lengths associated with the distribution function of the decoupled particles.

A program that bridges the microphysics of the production, evolution and decoupling of DM particles with large scale structure formation begins by obtaining the distribution function of the DM particles from the dynamics of production and decoupling. The DM distribution function determines the abundance [2], primordial phase space properties and generalized constraints on the DM candidate [38, 39] and their free streaming lengths [37]. Results in this direction have been reported [39, 40]. The primordial phase space density of particles \mathcal{D} permits to obtain deep insights on DM [39]. The phase space density can only decrease during gravitational dynamics via mergers and “violent relaxation” [41]. Recent photometric and kinematic data on dwarf spheroidal satellite galaxies in the Milky Way (dShps) and the observed DM density today yield upper and lower bounds on the mass, primordial phase space densities and velocity dispersion of the DM candidates [39]. Combining these constraints with recent results from N -body simulations yield estimates on the mass of the DM particles in the **range of a few keV** [39].

The DM distribution function after freeze-out is the main ingredient to obtain the transfer function and the power spectrum in the linear theory. In principle the DM transfer function may be obtained by modifying the publicly available CMB anisotropy codes [42, 43] that treat baryons, photons and dark matter [44], to account for the different distribution functions of several species and range of parameters, masses and couplings.

In practice, this is a computationally daunting problem: fairly complicated non-equilibrium distribution functions for a variety of possible DM species (axions, sterile neutrinos, etc) must be input in the codes (with substantial modifications of the standard codes). The exploration of the parameter space (masses, couplings and mixing angles) and their impact on the transfer function would require an enormous computational effort.

After matter-radiation equality, the contribution from the baryon-photon fluid to the DM transfer function can only be a few percent [1]. DM only couples to the baryon-photon fluid via gravitational interaction and the most prominent feature of this coupling on the DM transfer function are baryon acoustic oscillations (BAO) on a scale corresponding to the sound horizon at recombination, corresponding today to about 150 Mpc [45, 46, 47]. Our goal is to understand the (DM) transfer function at much *smaller* scales $\lambda \lesssim$ Mpc, at which the effect of the acoustic oscillations of the baryon-photon fluid (BAO) can be safely neglected.

Objectives: The main goals of this article are the following:

(a): to provide an *analytic, accurate and simple* framework to obtain the DM transfer function during matter domination for general initial conditions and *arbitrary distribution functions* of relic DM particles that decoupled in or out of LTE and that are *non-relativistic* after matter-radiation equality. Neglecting the gravitational coupling to

the baryon-photon fluid entails that the DM transfer function will eventually require corrections at the few percent level. However, we seek to gain understanding of robust features of $T(k)$ at small scales.

(b): to understand the impact of the statistics of the relic particle on the small scale properties of the transfer function. More precisely, we study which features of the distribution function affect more prominently the power spectrum at small scales.

Summary of Results: We study the linearized collisionless Boltzmann-Vlasov equation in the non-relativistic limit for particles that decoupled in or out of LTE with arbitrary (but isotropic) distribution functions and general initial conditions.

It is transformed into an integro-differential equation for density perturbations which features non-local kernels that include *memory of gravitational clustering* and represent corrections to the fluid description.

The influence of this memory becomes more important at *small scales*. Fermi-Dirac (FD) and Bose-Einstein (BE) statistics result in *long range* memory, with the longer range for Bose-Einstein statistics. Distribution functions that favor small momenta lead to longer range memory and result in an *enhancement of the transfer function at small scales*.

We obtain an *exact* expression for $T(k)$ for *arbitrary initial conditions and distribution functions* and provide a Fredholm expansion that systematically includes the effects of memory of gravitational clustering and higher moments of the distribution function, which are corrections to the fluid approximation.

An exhaustive numerical study of thermal relics that decoupled relativistically, (Fermions (FD) and Bosons, (BE)) or non-relativistically [WIMPs, (MB)] for different initial conditions reveal that the first two terms of the Fredholm series, given by eqn. (2.111) provide an accurate and simple approximation to the exact transfer function. These include explicitly the corrections to the fluid description and the influence of statistics on small scales. This approximation furnishes a useful tool to extract the broad properties of the transfer functions for arbitrary initial conditions and distribution functions.

The approximate expression for the transfer function given by eq.(2.111) features three main ingredients: **(i):** the solutions of Jeans' fluid equations, **(ii):** the free streaming solution of the Boltzmann equation *in absence of gravitational perturbations*, **(iii):** a non-local kernel that depends on the distribution function of the decoupled particles, it defines the second contribution in eq.(2.111), includes *memory* of gravitational clustering and represents a correction beyond the fluid approximation.

The scale of suppression of $T(k)$ is the comoving free streaming wave-vector at matter-radiation equality, $k_{fs}(t_{eq})$, where

$$k_{fs}(t) = \sqrt{\frac{4\pi\rho_{0M}a(t)}{\langle \frac{\vec{p}^2}{m^2} \rangle}}, \quad (1.1)$$

and the angular brackets refer to the average with the distribution function of the decoupled particle, ρ_{0M} is the DM matter density today and $a(t)$ the scale factor.

We find,

$$k_{fs}(t_{eq}) = \begin{cases} \frac{5.88}{\text{pc}} \left(\frac{g_d}{2}\right)^{\frac{1}{3}} \left(\frac{m}{100 \text{ GeV}}\right)^{\frac{1}{2}} \left(\frac{T_d}{10 \text{ MeV}}\right)^{\frac{1}{2}} & \text{WIMPs} \\ 0.00284 \left(\frac{g_d}{2}\right)^{\frac{1}{3}} \frac{m}{\text{keV}} [\text{kpc}]^{-1} & \text{FD thermal relics} \\ 0.00317 \left(\frac{g_d}{2}\right)^{\frac{1}{3}} \frac{m}{\text{keV}} [\text{kpc}]^{-1} & \text{BE thermal relics} \end{cases} \quad (1.2)$$

where g_d is the number of relativistic species at decoupling.

For large scales $k \lesssim k_{fs}(t_{eq})$, the contribution of the non-local memory kernel is subleading, whereas for scales $k > k_{fs}(t_{eq})$ the memory of gravitational clustering and corrections beyond the fluid approximation become important.

FD and BE distribution functions lead to long range memory kernels with Bose-Einstein statistics leading to the longest range. Longer range memory leads to an enhancement of the transfer function (and power spectrum) at *small scales* as depicted in fig. 10. For $k > k_{fs}(t_{eq})$, ($\gamma > \sqrt{2}$) the difference in statistics of the decoupled particles becomes very important

At large scales $k \ll k_{fs}(t_{eq})$ the transfer function $T(k)$ in terms of the variable $\gamma = \sqrt{2} k/k_{fs}(t_{eq})$ has the following behaviour for all cases considered

$$T(k) = 1 - \left(\frac{\gamma}{\gamma_0}\right)^2 + \mathcal{O}(\gamma^4) \quad (1.3)$$

where γ_0 is the same for Fermi-Dirac, Bose-Einstein and Maxwell-Boltzmann distribution functions, and is given by eq.(3.21).

The transfer function for the three different cases (MB, FD and BE) can be compared by parametrizing them in terms of γ . This comparison for different initial conditions is displayed in fig. 10. Simple functional fits to $T(k)$ are provided on different regions of k for various initial conditions for thermal relics.

II. GILBERT'S EQUATION

After decoupling from the plasma, or freeze-out, the distribution function of the decoupled particles obeys the collisionless Boltzmann-equation. In absence of gravitational perturbations the solution of this equation yields a distribution function of the form [2, 39]

$$f_0(P_f(t), t) = f_0\left(P_f(t) \frac{a(t)}{a_d}\right) = f_0(p), \quad (2.1)$$

where $P_f(t)$, $a(t)$, a_d are the physical momentum, scale factor and its value at decoupling respectively, and \vec{p} is the comoving momentum. Consistently with isotropy we assume that f_0 is a function of $p = |\vec{p}|$.

During the matter dominated era, for modes that are deep inside the Hubble radius and DM particles that are non-relativistic the evolution of DM density perturbations and gravitational perturbations is studied with the non-relativistic Boltzmann-Vlasov equation[24]. The non-relativistic case applies to all comoving scales (physical scales today) $\lambda \lesssim 170$ Mpc which were inside the Hubble radius at matter-radiation equality and DM particles with masses $m >$ few eV that decoupled before matter-radiation equality.

To linear order in perturbations the distribution function of the decoupled particle and the Newtonian gravitational potential are [1, 24, 25]

$$f(\vec{p}; \vec{x}; t) = f_0(p) + F_1(\vec{p}; \vec{x}; t) \quad (2.2)$$

$$\varphi(\vec{x}, t) = \varphi_0(\vec{x}, t) + \varphi_1(\vec{x}, t), \quad (2.3)$$

where $f_0(p)$ is the unperturbed distribution function of the decoupled particle, $\varphi_0(\vec{x}, t)$ is the background gravitational potential that determines the homogeneous and isotropic Friedmann-Robertson-Walker metric and \vec{p}, \vec{x} are comoving variables.

The reader is referred to refs. [1, 23, 25, 29, 30, 31] for details on the linearization of the non-relativistic collisionless Boltzmann-Vlasov equation.

In conformal time τ and in terms of comoving variables \vec{p}, \vec{x} the linearized Boltzmann-Vlasov equation is [23, 29, 30]

$$\frac{1}{a} \frac{\partial F_1}{\partial \tau} + \frac{\vec{p}}{m a^2} \cdot \vec{\nabla}_{\vec{x}} F_1 - m \vec{\nabla}_{\vec{x}} \varphi_1 \cdot \vec{\nabla}_{\vec{p}} f_0 = 0, \quad (2.4)$$

along with Poisson's equation,

$$\nabla_{\vec{x}}^2 \varphi_1 = \frac{4 \pi G m}{a} \int \frac{d^3 p}{(2\pi)^3} F_1(\vec{x}, \tau). \quad (2.5)$$

It is convenient [29, 30] to introduce a new time variable s related to the conformal time τ by

$$ds = \frac{d\tau}{a}, \quad (2.6)$$

and to take spatial Fourier transforms of the gravitational potential $\varphi_1(\vec{x}, \tau)$ and the perturbation $F_1(\vec{x}, \tau)$ to obtain

$$\frac{\partial F_1(\vec{k}, \vec{p}; s)}{\partial s} + \frac{i \vec{k} \cdot \vec{p}}{m} F_1(\vec{k}, \vec{p}; s) - i \vec{k} \cdot \vec{\nabla}_{\vec{p}} f_0(p) a^2(s) \varphi_1(\vec{k}, s) = 0 \quad (2.7)$$

where

$$\varphi_1(\vec{k}; s) = -\frac{4 \pi G m}{k^2 a(s)} \int \frac{d^3 p}{(2\pi)^3} F_1(\vec{k}, \vec{p}; s) \quad (2.8)$$

Integrating from the initial time $s = s_i$ to s , the Boltzmann-Vlasov equation (2.7) yields

$$F_1(\vec{k}, \vec{p}; s) = F_1(\vec{k}, \vec{p}; s_i) e^{-i \frac{\vec{k} \cdot \vec{p}}{m} (s - s_i)} + i m \vec{k} \cdot \vec{\nabla}_{\vec{p}} f_0(p) \int_{s_i}^s ds' e^{-i \frac{\vec{k} \cdot \vec{p}}{m} (s' - s_i)} a^2(s') \varphi_1(\vec{k}, s'). \quad (2.9)$$

This equation can be turned into an integral equation for the gravitational potential by multiplying both sides by $-4\pi G m/[k^2 a(s)]$, integrating in \vec{p} , and using the relation (2.8). We obtain

$$\varphi_1(\vec{k}; s) + i \frac{4\pi G m^2}{k^2 a(s)} \int \frac{d^3 p}{(2\pi)^3} \vec{k} \cdot \vec{\nabla}_{\vec{p}} f_0(p) \int_{s_i}^s ds' e^{-i \frac{\vec{k} \cdot \vec{p}}{m} (s-s_i)} a^2(s') \varphi_1(\vec{k}, s') = -\frac{4\pi G m}{k^2 a(s)} \int \frac{d^3 p}{(2\pi)^3} F_1(\vec{k}, \vec{p}; s_i) e^{-i \frac{\vec{k} \cdot \vec{p}}{m} (s-s_i)}. \quad (2.10)$$

The right hand side of this equation, the inhomogeneity, is determined by the first term in the solution eq.(2.9) and describes the *free streaming* solution of the Boltzmann-equation in absence of gravitational perturbations. This can be seen directly by performing the inverse Fourier transform in \vec{k} to spatial coordinates, which yields for the inhomogeneity the following form:

$$\int \frac{d^3 p}{(2\pi)^3} \mathcal{F}[\vec{x} - \frac{\vec{p}}{m}(s - s_i)] \quad \text{where} \quad \mathcal{F}[\vec{x}] = -\frac{4\pi G m}{a(s)} \int e^{i \vec{k} \cdot \vec{x}} F_1(\vec{k}, \vec{p}; s_i) \frac{d^3 k}{k^2}. \quad (2.11)$$

For a species that has become non-relativistic: $\vec{p}/m = \vec{v}$ where \vec{v} is the comoving velocity. Using the relation eq.(2.6) and $d\tau = dt/a(t)$ we see that

$$\frac{p}{m} (s - s_i) = \int_{t_i}^t \frac{v(t')}{a(t')} dt' \equiv l_{fs}(v; t) \quad (2.12)$$

where $v(t) = v/a(t)$ is the physical velocity of the non-relativistic particle and $l_{fs}(v; t)$ is the *comoving* free streaming distance that the particle with comoving velocity v has traveled during (comoving) time from t_i until t [2]. The physical distance is obtained by multiplying the above expression by $a(t)$. Therefore the inhomogeneity eq.(2.11) in eq.(2.10) is of the form

$$\int \frac{v^2 dv}{2\pi^2} \mathcal{F}[x - l_{fs}(v; t)].$$

The variable s , related to conformal time as in eq.(2.6), obeys the differential equation

$$\frac{ds}{da} = \frac{1}{a^3 H(a)}, \quad (2.13)$$

where a is the scale factor and H the Hubble parameter. For matter dominated cosmology

$$H(a) = \frac{H_{0M}}{a^{\frac{3}{2}}}, \quad (2.14)$$

where

$$H_{0M}^2 = \frac{8\pi G}{3} \rho_{0M} \equiv H_0^2 \Omega_M, \quad (2.15)$$

with $H_0 = 100 h \text{ km sec}^{-1} \text{ Mpc}^{-1}$ is the Hubble parameter *today* and ρ_{0M} is the matter density *today* with $\Omega_M = 0.233$ for DM.

Normalizing the scale factor to unity *today*, namely $a(0) = 1$ and taking $s_i = 0$ as initial value for the time variable s , eq.(2.13) is integrated to yield

$$s = \frac{2}{H_{0M} a_i^{\frac{1}{2}}} \left[1 - \left(\frac{a_i}{a} \right)^{\frac{1}{2}} \right]. \quad (2.16)$$

The initial value of the scale factor a_i corresponds to the value at matter-radiation equality $a_i = a_{eq} = 1/(1 + z_{eq})$ with $z_{eq} \simeq 3050$. It is convenient to introduce a dimensionless time variable u as

$$s = \frac{2u}{H_{0M} a_{eq}^{\frac{1}{2}}}, \quad (2.17)$$

so that

$$u = 1 - \left(\frac{a_{eq}}{a} \right)^{\frac{1}{2}} = 1 - \sqrt{\frac{1+z}{1+z_{eq}}}, \quad 0 \leq u \leq 1 - a_{eq}^{\frac{1}{2}} \simeq 0.982 \quad (2.18)$$

and the scale factor in terms of the variable u is

$$a(u) = \frac{a_{eq}}{(1-u)^2}. \quad (2.19)$$

A. The free streaming length.

We note that during matter domination, the comoving free streaming distance is given by

$$l_{fs}(t) = v \int_{t_i}^t \frac{dt'}{a^2(t')} = \frac{v}{H_{0M}} \int_{t_i}^t \frac{da}{a^{\frac{3}{2}}} = \frac{2v}{H_{0M}} \left[\frac{1}{\sqrt{a_{eq}}} - \frac{1}{\sqrt{a(t)}} \right]. \quad (2.20)$$

We see that the second term in $l_{fs}(t)$ scales as $1/\sqrt{a(t)}$. This observation will be important below to establish the redshift dependence of the *comoving* free streaming wave-vector.

Motivated by the expression for the free-streaming distance eq.(2.12) and (2.20) and by the usual Jeans' wavevector for fluids [24], we introduce the *physical* free streaming wavevector,

$$k_{p,fs}(t) = \frac{k_{fs}(t)}{a(t)}. \quad (2.21)$$

The *comoving* free streaming wavevector is defined as

$$k_{fs}^2(t) = \frac{3 H_{0M}^2 a(t)}{2 \langle \vec{V}^2 \rangle} = a^2(t) \frac{4 \pi G \rho_M(t)}{\langle \vec{V}^2(t) \rangle}, \quad \rho_M(t) = \frac{\rho_{0M}}{a^3(t)}, \quad \langle \vec{V}^2(t) \rangle = \frac{\langle \vec{V}^2 \rangle}{a^2(t)}. \quad (2.22)$$

This definition of the free streaming wavevector is analogous to that of the Jeans' wavevector in a fluid replacing the speed of sound by $\sqrt{\langle \vec{V}^2 \rangle}$ (see the discussion below).

It is clear from this expression that the comoving free streaming wave vector scales as

$$k_{fs}(t) = k_{fs}(0) \sqrt{a(t)}, \quad (2.23)$$

where, using eq.(2.22),

$$k_{fs}(0) = \sqrt{\frac{3 H_{0M}^2}{2 \langle \vec{V}^2 \rangle}}. \quad (2.24)$$

The comoving free streaming wavelength is given by:

$$\lambda_{fs}(t) \equiv \frac{2 \pi}{k_{fs}(t)}. \quad (2.25)$$

There is a simple interpretation of $k_{fs}(t_i)$: consider the comoving free streaming distance that a particle with comoving velocity $v = \sqrt{\langle \vec{V}^2 \rangle}$ travels from the initial time $t_i = t_{eq}$ until today. Setting $s = 0$ in eq.(2.20) and neglecting the second term since $1/\sqrt{a(0)} = 1 \ll 1/\sqrt{a_{eq}} \simeq 55.2$, we find

$$l_{fs}(v; 0) = \frac{2 \sqrt{\langle \vec{V}^2 \rangle}}{H_{0M} a_i^{\frac{1}{2}}}. \quad (2.26)$$

Therefore,

$$k_{fs}(t_{eq}) = 0.0181 k_{fs}(0) = \frac{\sqrt{6}}{l_{fs}(v; 0)} \Rightarrow \lambda_{fs}(t_{eq}) = \sqrt{\frac{2}{3}} \pi l_{fs}(v; 0), \quad (2.27)$$

We note that the free streaming wavevector at t_{eq} is related to the free streaming distance that the particle has traveled between matter-radiation equality and today.

The matter density *today* is ¹

$$\rho_{0M} = m n_0, \quad n_0 = \int \frac{d^3 p}{(2\pi)^3} f_0(p). \quad (2.28)$$

¹ We consider a species with a single internal degree of freedom, a different value g can easily be included in the final expressions.

It also proves convenient to introduce the density perturbation

$$\Delta(\vec{k}, s) = m \int \frac{d^3 p}{(2\pi)^3} F_1(\vec{k}, \vec{p}; s), \quad (2.29)$$

related to the gravitational potential as

$$\varphi_1(\vec{k}; s) a(s) = -\frac{4\pi G}{k^2} \Delta(\vec{k}; s), \quad (2.30)$$

and the gravitational potential normalized at the initial time

$$\Phi(\vec{k}, u) = \frac{\varphi_1(\vec{k}, s)}{\varphi_1(\vec{k}, 0)}, \quad (2.31)$$

where $s(u)$ is given by eq.(2.17).

The unperturbed distribution function $\tilde{f}_0(p)$ is a dimensionless function, and as such it can be written as a function of the ratio of the comoving momentum p and the value of the decoupling temperature *today* $T_{d,0}$ and other dimensionless quantities, such as the ratio of the mass of the particle to the decoupling temperature, dimensionless coupling constants from the microphysics of decoupling etc., [2, 39], namely

$$f_0(p) \equiv f_0(y; x_1, x_2 \dots) \quad , \quad y = \frac{p}{T_{d,0}} \quad , \quad x_1 = \frac{m}{T_d} \dots \quad , \quad (2.32)$$

where T_d is the decoupling temperature and $T_{d,0} = T_d a_d$ is its value *today*. Using entropy conservation it follows that [2]

$$T_{d,0} = \left(\frac{2}{g_d}\right)^{\frac{1}{3}} T_{cmb}, \quad (2.33)$$

where $T_{cmb} = 2.348 \times 10^{-4}$ eV is the CMB temperature today and g_d is the effective number of relativistic degrees of freedom at decoupling. For these distributions

$$n_0 = T_{d,0}^3 \int_0^\infty \frac{dy}{2\pi^2} y^2 f_0(y).$$

Integrating by parts the momentum integral in the left hand side of eq.(2.10), integrating over the angle $\hat{k} \cdot \hat{p} = \cos \theta$ and dividing both sides of the integral equation (2.10) by the initial value

$$\varphi_1(\vec{k}; 0) = -\frac{4\pi G m}{k^2 a_{eq}} \int \frac{d^3 p}{(2\pi)^3} F_1(\vec{k}, \vec{p}; 0), \quad (2.34)$$

the integral equation (2.10) becomes

$$\Phi(k, u) - \frac{6}{\alpha} (1-u)^2 \int_0^u \Pi[\alpha(u-u')] \frac{\Phi(k, u')}{[1-u']^4} du' = (1-u)^2 I[\alpha u]. \quad (2.35)$$

where

$$\alpha \equiv \frac{2k}{H_0 \Omega_M^{\frac{1}{2}} a_i^{\frac{1}{2}}} \frac{T_{d,0}}{m}. \quad (2.36)$$

Using eq.(2.33) and the value

$$\Omega_M h^2 = 0.105 \quad (2.37)$$

for non-baryonic dark matter, α becomes

$$\alpha = 240 \left(\frac{2}{g_d}\right)^{\frac{1}{3}} \frac{\text{keV}}{m} k \text{ kpc}. \quad (2.38)$$

The cosmologically relevant range where this approach applies goes from scales well inside the Hubble radius (where the non-relativistic approximation is valid) till the smallest scales where the linearized approximations are valid

$$(1000 \text{ Mpc})^{-1} \lesssim k \lesssim (0.01 \text{ Mpc})^{-1} . \quad (2.39)$$

Therefore, the range of the dimensionless variable α results as

$$0.24 \cdot 10^{-3} \left(\frac{2}{g_d} \right)^{\frac{1}{3}} \frac{\text{keV}}{m} \lesssim \alpha \lesssim 24 \left(\frac{2}{g_d} \right)^{\frac{1}{3}} \frac{\text{keV}}{m} . \quad (2.40)$$

As it is customary, we only consider distributions spherically symmetric on \vec{k} . The non-local kernel in eqn. (2.35) is given by

$$\Pi[z] = \int_0^\infty dy y \tilde{f}_0(y) \sin[yz] , \quad (2.41)$$

where we introduced the normalized distribution function

$$\tilde{f}_0(y) \equiv \frac{f_0(y)}{\int_0^\infty dy y^2 f_0(y)} ; \quad \int_0^\infty y^2 \tilde{f}_0(y) dy = 1 , \quad (2.42)$$

and

$$I[\alpha u] = \frac{1}{\int_0^\infty p^2 dp F_1(k, p; 0)} \int_0^\infty p^2 dp F_1(k, p; 0) \frac{\sin\left(\frac{\alpha p u}{T_{d,0}}\right)}{\left(\frac{\alpha p u}{T_{d,0}}\right)} , \quad (2.43)$$

where we have assumed that F_1 does not depend on the direction of \vec{p} .

The inhomogeneity $I[\alpha u]$ obeys the initial conditions

$$I[\alpha u = 0] = 1 \quad , \quad \left. \frac{d}{du} I[\alpha u] \right|_{u=0} = 0 . \quad (2.44)$$

The density perturbation normalized at the initial time namely

$$\delta(k, u) = \frac{\Delta(k; s)}{\Delta(k; 0)} \quad (2.45)$$

is related to $\Phi(k; u)$ [see eq.(2.30) and eq.(2.19)] by

$$\Phi(k; u) = \frac{a_{eq}}{a(u)} \delta(k, u) = (1 - u)^2 \delta(k, u) . \quad (2.46)$$

Then, from eq.(2.35) $\delta(k, u)$ obeys the Volterra equation of the second kind

$$\delta(k, u) - \frac{6}{\alpha} \int_0^u \Pi[\alpha(u - u')] \frac{\delta(k, u')}{[1 - u']^2} du' = I[\alpha u] . \quad (2.47)$$

which is Gilbert's equation[29].

The initial conditions of the inhomogeneity eq.(2.44) lead to the following initial conditions on the gravitational potential and density perturbations

$$\delta(k, u = 0) = 1 \quad , \quad \left. \frac{d}{du} \delta(k, u) \right|_{u=0} = 0 \quad (2.48)$$

$$\Phi(k, u = 0) = 1 \quad , \quad \left. \frac{d}{du} \Phi(k, u) \right|_{u=0} = -2 . \quad (2.49)$$

B. Exact results from Gilbert's equation

The long wavelength limit $\alpha \rightarrow 0$ of eq.(2.47) affords an exact solution. In this limit,

$$\lim_{\alpha \rightarrow 0} \frac{1}{\alpha} \Pi[\alpha(u-u')] = u-u' \quad , \quad I[0] = 1 \quad , \quad (2.50)$$

and $(u-u') \Theta(u-u')$ is the Green's function of the differential operator d^2/d^2u . Therefore taking the second derivative with respect to u of the Volterra equation (2.47), we obtain

$$\ddot{\delta}(0, u) - \frac{6}{(1-u)^2} \delta(0, u) = 0 \quad , \quad (2.51)$$

the solution satisfying the initial conditions eq.(2.48) is

$$\delta(0, u) = \frac{3}{5} \frac{1}{(1-u)^2} + \frac{2}{5} (1-u)^3 \quad , \quad (2.52)$$

which in terms of the scale factor eq.(2.19) is given by

$$\delta(0, u) = \frac{3}{5} \frac{a(u)}{a_{eq}} + \frac{2}{5} \left[\frac{a_{eq}}{a(u)} \right]^{\frac{3}{2}} \quad . \quad (2.53)$$

This is the usual long-wavelength solution for density perturbations in a matter dominated cosmology. From the eq.(2.46) the long-wavelength limit of the gravitational potential is

$$\Phi(0, u) = \frac{3}{5} + \frac{2}{5} (1-u)^5 \quad . \quad (2.54)$$

We now show that $\delta(k, u)$ behaves as $1/(1-u)^2$ for all values of α when $u \rightarrow 1$.

Let us assume a general power law behavior for $\delta(k, u)$ as $u \rightarrow 1$,

$$\delta(k, u) \stackrel{u \rightarrow 1}{\cong} A(\alpha) (1-u)^{-\beta} [1 + \mathcal{O}(1-u)] \quad . \quad (2.55)$$

For $u \rightarrow 1$ the integral in eq.(2.47) is dominated by the region $u' \sim u \sim 1$, and we note that

$$\Pi[\alpha(u-u')] \stackrel{u' \rightarrow u}{\cong} \alpha(u-u') \quad . \quad (2.56)$$

In this limit we obtain

$$\frac{6}{\alpha} \int_0^u \frac{\Pi[\alpha(u-u')]}{[1-u']^2} (1-u')^{-\beta} du' \stackrel{u \rightarrow 1}{\cong} \frac{6}{\beta(\beta+1)} (1-u)^{-\beta} \quad . \quad (2.57)$$

Inserting this result in eq.(2.47) we find two solutions: $\beta = 2, -3$ which are precisely the singular and regular solutions found in the long-wavelength limit [1]. Therefore, the dominant behavior for $u \rightarrow 1$ for *all* values of α is

$$\delta(k, u) \stackrel{u \rightarrow 1}{\cong} \frac{A(\alpha)}{(1-u)^2} = A(\alpha) \frac{a(u)}{a_{eq}} \quad (2.58)$$

$$\Phi(k, u) \stackrel{u \rightarrow 1}{\cong} A(\alpha) \quad (2.59)$$

where in order to find the function $A(\alpha)$ we have to integrate the Gilbert equation from $u = 0$, where the initial conditions were defined, up to $u \rightarrow 1$. $\Phi(k, u)$ is a *slowly* varying function of u in the sense that it is always finite as we see from eq.(2.59).

The transfer function: $T(k)$ is defined from the limit [1]

$$\lim_{u \rightarrow 1} \frac{a_{eq}}{a(u)} \frac{\delta(k, u)}{\delta(k, 0)} = \lim_{u \rightarrow 1} \Phi(k, u) \quad , \quad (2.60)$$

where we have used the relation eq.(2.46) and the initial condition eq.(2.48). It is customary to normalize the transfer function so that $T(k) \rightarrow 1$ as $k \rightarrow 0$, obtaining

$$T(k) \equiv \lim_{u \rightarrow 1} \frac{\Phi(k, u)}{\Phi(0, u)} = \frac{5}{3} \lim_{u \rightarrow 1} (1 - u)^2 \delta(k, u) = \frac{5}{3} \Phi(k, u = 1) = \frac{5}{3} A(\alpha). \quad (2.61)$$

A numerical study of $\delta(k, u)$ and $T(k)$ depicted in figs. 1-5, 7, 9-10 show that $T(k)$ decreases with k (or α). This is to be expected, $k = 0$ corresponds to the mode that grows the fastest as it is the most gravitationally unstable, larger values of k result in slower growth as a consequence of free streaming. The behaviour of the $k = 0$ mode is that of cold dark matter eq.(2.52).

Therefore, $T(k)$ is a measure of the suppression of the $k > 0$ wave modes and the k -scale of suppression of $T(k)$ is necessarily related to the free-streaming wavenumber.

The final power spectrum $P_f(k)$ is related to the initial one $P_i(k)$ as [1]

$$P_f(k) = T^2(k) P_i(k). \quad (2.62)$$

If perturbations do not grow or decay substantially during the prior, radiation dominated phase, $P_i(k)$ is nearly the inflationary primordial power spectrum [1].

Gilbert's equation (2.47) can be solved in a power series in u , appropriate for short times. We find from eq.(2.43)

$$I[\alpha u] \stackrel{u \rightarrow 0}{\approx} 1 - b \alpha^2 u^2 + \mathcal{O}(u^4) \quad , \quad b \equiv \frac{1}{6 T_{d,0}^2} \frac{\int_0^\infty p^4 dp F_1(k, p; 0)}{\int_0^\infty p^2 dp F_1(k, p; 0)} \quad (2.63)$$

Thus, we find from eqs.(2.63) and (2.47),

$$\delta(k, u) \stackrel{u \rightarrow 0}{\approx} 1 + u^2 [3 - b \alpha^2] + \mathcal{O}(u^4) \quad (2.64)$$

Therefore $\delta(k, u)$ starts out by growing or decreasing for small u depending on whether $\alpha < \alpha_c$ or $\alpha > \alpha_c$, respectively, where

$$\alpha_c = \sqrt{\frac{3}{b}}.$$

Namely, for $\alpha < \alpha_c$ the mode $\delta(k, u)$ is gravitationally unstable from the start ($u = 0$) while for $\alpha > \alpha_c$ the mode starts being gravitationally stable. However, due to the cosmological expansion all modes redshift and eventually become gravitationally unstable at some time $u < 1$. As can be seen from eq.(2.58), for $u \rightarrow 1$ **all** modes are unstable.

At early times, α_c determines the stability limit of density perturbations.

We carried out an exhaustive numerical study for cold, hot and warm dark matter (Maxwellian (MB), BE and FD distributions). We find for large α that $T(k)$ decreases exponentially in the Maxwell-Boltzmann case while for both bosons and fermions $T(k)$ asymptotically decreases with a power law or exponentially (see below secs. IV A and IV B).

At different scales, the suppression of $T(k)$ is described by a characteristic wave vector k_{char} which depends on the initial conditions, the particle statistics and the regime of wavenumbers.

We obtain k_{char} from the numerical study for different cases and k regimes, in all cases considered we find that $k_{char} \sim k_{fs}(t_{eq})$.

C. Thermal and Gilbert's initial conditions

It remains to specify the initial perturbation $F_1(k, p; u = 0)$ of the distribution function. Although in principle this function should be obtained from the full evolution through the prior radiation dominated stage, in what follows we consider the physically motivated case of adiabatic perturbations for which the perturbation $F_1(k, p; u = 0)$ corresponds to a temperature perturbation,

$$T_{d,0} \rightarrow T_{d,0} \left[1 + \frac{\Delta T(k)}{T_{d,0}} \right],$$

namely,

$$F_1(k, p; u = 0) = T \frac{df_0(p, T)}{dT} \frac{\Delta T(k)}{T}. \quad (2.65)$$

These are the initial conditions proposed in refs.[21, 23]. Alternative initial conditions were proposed by Gilbert [29], who chose

$$F_1(k, p; u = 0) = f_0(p) C(k), \quad (2.66)$$

with some unspecified function $C(k)$.

D. Solution of the Gilbert equation in powers of k .

We can solve the Gilbert equation (2.47) in powers of α^2 , [that is, powers of k^2 , see eq.(2.36)]

$$\delta(k, u) = \delta_0(u) + \alpha^2 \delta_1(u) + \mathcal{O}(\alpha^4), \quad (2.67)$$

where $\delta_0(u)$ is given by eq.(2.52) and $\delta_1(0) = \delta_1'(0) = 0$. Inserting eq.(2.67) in eq.(2.47), using eq.(2.63) and deriving twice with respect to u leads to the equation

$$\left[\frac{d^2}{du^2} - \frac{6}{(1-u)^2} \right] \delta_1(u) = 2 [3b - \bar{b} - 3b \delta_0(u)]$$

where $\bar{b} = b$ for Gilbert initial conditions and $\bar{b} = \frac{5}{3} b$ for temperature initial conditions. This inhomogeneous differential equation for $\delta_1(u)$ can be easily solved using the Green's function of the differential operator in the l. h. s. We find for $u \rightarrow 1$ after calculation,

$$\delta_1(u) \stackrel{u \rightarrow 1}{\equiv} \begin{cases} -\frac{8b}{35} \frac{1}{(1-u)^2} + \mathcal{O}(1) & \text{Gilbert initial conditions,} \\ -\frac{31b}{105} \frac{1}{(1-u)^2} + \mathcal{O}(1) & \text{Temperature initial conditions.} \end{cases} \quad (2.68)$$

Using eq.(2.61) we now obtain $T(k)$ in powers of α^2 ,

$$T(k) = \begin{cases} 1 - \frac{8b}{21} \alpha^2 + \mathcal{O}(\alpha^4) & \text{Gilbert initial conditions,} \\ 1 - \frac{31b}{63} \alpha^2 + \mathcal{O}(\alpha^4) & \text{Temperature initial conditions,} \end{cases} \quad (2.69)$$

where b is given by eqn. (2.63).

E. Gilbert's equation as an integro-differential equation.

The results obtained above suggest to convert the Volterra equation into an integro-differential equation. Taking the second derivative with respect to u of eq.(2.47) yields

$$\ddot{\delta}(k, u) - \frac{6 \delta(k, u)}{(1-u)^2} + 6 \alpha^2 \int_0^u du' \int_0^\infty dy y^4 \tilde{f}_0(y) \frac{\sin[\alpha y (u - u')]}{\alpha y} \frac{\delta(k, u')}{(1-u')^2} = \ddot{I}[k, u]. \quad (2.70)$$

It proves convenient to write the following identity in the y -integral:

$$y^4 = y^2 \overline{y^2} + y^2 (y^2 - \overline{y^2}), \quad (2.71)$$

where

$$\overline{y^2} = \int_0^\infty dy y^4 \tilde{f}_0(y) \quad \text{with} \quad \int_0^\infty dy y^2 \tilde{f}_0(y) = 1, \quad (2.72)$$

and to introduce

$$3 \gamma^2 \equiv \alpha^2 \overline{y^2} \quad , \quad \gamma = \frac{2k T_{d,0}}{m H_0} \sqrt{\frac{\overline{y^2}}{3 \Omega_M a_{eq}}}, \quad (2.73)$$

where eq.(2.36) was used.

In terms of k_{fs} [see eqs.(2.15), (2.24) and (2.73)] we find that

$$\gamma^2 = \frac{2 k^2}{k_{fs}^2(t_{eq})} = \frac{2 k^2}{k_{fs}^2(0) a_{eq}} \quad , \quad k_{fs}(0) = \sqrt{\frac{3 \Omega_M}{2 y^2}} H_0 \frac{m}{T_{d,0}} . \quad (2.74)$$

Using the original eq.(2.47) to replace the term with $\overline{y^2}$ in terms of $\delta(k, u)$ and $I[\alpha u]$, we obtain the following integro-differential equation for density perturbations

$$\ddot{\delta}(k, u) - \frac{6 \delta(k, u)}{(1-u)^2} + 3 \gamma^2 \delta(k, u) - \int_0^u du' K(u-u') \frac{\delta(k, u')}{(1-u')^2} = \ddot{I}[k, u] + 3 \gamma^2 I[\alpha u] , \quad (2.75)$$

where the non-local kernel $K(u-u')$ is given by

$$K(u-u') = 6 \alpha \int_0^\infty y (\overline{y^2} - y^2) \tilde{f}_0(y) \sin[\alpha y (u-u')] dy . \quad (2.76)$$

and we note that

$$\overline{y^2} \left(\frac{T_{d,0}}{m} \right)^2 = \langle \vec{V}^2 \rangle \quad (2.77)$$

is the three dimensional velocity dispersion of the non-relativistic particles *today*.

Using eq.(2.26), γ [eq.(2.73)] can also be written as

$$\gamma = \frac{\sqrt{2} k}{k_{fs}(t_{eq})} = \frac{1}{\sqrt{3}} k l_{fs}(v; 0) = \frac{2 \pi}{\sqrt{3}} \frac{l_{fs}(v; 0)}{\lambda} , \quad (2.78)$$

where λ is the wavelength of the perturbation.

Using eqs.(2.24), (2.33) and (2.37), $k_{fs}(t_{eq})$ and $l_{fs}(v; 0)$ are given by

$$k_{fs}(t_{eq}) = \frac{0.0102}{\sqrt{\overline{y^2}}} \left(\frac{g_d}{2} \right)^{\frac{1}{3}} \frac{m}{\text{keV}} [\text{kpc}]^{-1} \quad (2.79)$$

$$\lambda_{fs}(t_{eq}) = \sqrt{\frac{2}{3}} \pi l_{fs}(v; 0) = 616 \sqrt{\overline{y^2}} \left(\frac{2}{g_d} \right)^{\frac{1}{3}} \frac{\text{keV}}{m} \text{ kpc} . \quad (2.80)$$

The transfer function for the three different cases (MB, FD and BE) turns to be parametrized by the dimensionless ratio $\gamma = \sqrt{2} k/k_{fs}(t_{eq})$ allowing us to compare the three different cases, in fig. 10 below.

The alternative form eq.(2.75) of the original Volterra (Boltzmann-Vlasov) [eq.(2.47)] equation has several merits :

- Neglecting the non-local term and the inhomogeneity, eq.(2.75) can be written in a more familiar form in terms of cosmic time t :

$$\frac{d^2 \delta}{dt^2} + 2 H \frac{d\delta}{dt} + \left[\frac{k^2 \langle \vec{V}^2 \rangle}{a^4(t)} - 4 \pi G \rho_M(t) \right] \delta = 0 \quad (2.81)$$

where $\langle \vec{V}^2 \rangle$ is given by eq.(2.77) and $\langle \vec{V}^2 \rangle / a^2(t)$ is the *physical* squared velocity of the non-relativistic particles.

The term between brackets in eq.(2.81) can be written as

$$\frac{\langle \vec{V}^2 \rangle}{a^2(t)} \left[\frac{k^2}{a^2(t)} - \frac{k_{fs}^2(t)}{a^2(t)} \right] \quad (2.82)$$

where $k_{fs}(t)$ is the *comoving* free streaming wavevector eq.(2.22). This equation must be compared to the usual fluid equation [24] in which the comoving Jeans wave vector $k_J(t)$ replaces $k_{fs}(t)$ with

$$k_J^2(t) = \frac{4 \pi G}{c_s^2} \rho_{0M} a(t) , \quad (2.83)$$

where c_s is the comoving speed of sound during matter domination. This expression shows that the *comoving* Jean's wavevector in the fluid description scales as $\sqrt{a(t)}$ during matter domination, just as the free streaming wavevector $k_{fs}(t)$ does. Thus, we see that the long-wavelength limit $\alpha \rightarrow 0$ ($\gamma \rightarrow 0$) of eq.(2.75) yields the familiar fluid description.

Therefore the contribution from the non-local kernel $K(u - u')$ is a *correction* to the fluid description. It will be seen below that this correction becomes important at small scales $k > k_{fs}(t_{eq})$.

- In the long wavelength limit $\alpha \rightarrow 0$ ($\gamma \rightarrow 0$) the kernel $K(u - u')$ decreases as $\gamma^4 \ll \gamma^2$ and its contribution to the dynamics of density perturbations becomes negligible.

Furthermore, expanding the kernel $K(u - u')$ in a power series in k it can be seen that each term corresponds to higher correlations of the form

$$\left\langle \left(\frac{p}{m} \right)^{2+n} \right\rangle - \left\langle \left(\frac{p}{m} \right)^n \right\rangle \left\langle \left(\frac{p}{m} \right)^2 \right\rangle .$$

These correlations are typically neglected in the moment-hierarchy of the Boltzmann equation [1].

- At short times $u \sim 0$ it follows that

$$\int_0^u K(u - u') du' \stackrel{u \rightarrow 0}{\approx} \mathcal{O}(\gamma^4 u^4) ,$$

hence, its contribution is subleading for $u \lesssim 1/\gamma$ since $\delta(k, u \sim 0) \sim 1$ by the initial condition.

- As $u \rightarrow 1$, the u' integral in the kernel is dominated by the region $u \sim u' \sim 1$ for which $\delta(k, u') \sim A(\alpha)/(1 - u')^2$ as obtained in eq.(2.58), therefore it follows that for $u \sim 1$,

$$\int_0^u du' K(u - u') \frac{\delta(k, u')}{(1 - u')^2} \stackrel{u \rightarrow 1}{\approx} \alpha^4 [\overline{y^4} - (\overline{y^2})^2] \ln \frac{1}{1 - u} \ll \frac{1}{(1 - u)^2} . \quad (2.84)$$

Therefore in this region the contribution of the kernel is subleading as compared to the first three terms in eq.(2.75) although it could be larger than the inhomogeneity on the right hand side.

- It explicitly yields the asymptotic behavior $\delta(k, u \rightarrow 1) \propto 1/(1 - u)^2$ as a consequence of the second term in eq.(2.75) and the analysis above. This feature will be seen manifestly in the analysis below.

F. The *exact* transfer function and its Fredholm expansion.

The above analysis points out that in all the regimes of interest the non-local contribution from the kernel is small as compared to the first three terms in the eq.(2.75) and can be treated perturbatively. For this purpose, it is convenient to write eq.(2.75) as

$$\ddot{\delta}(k, u) - \frac{6}{(1 - u)^2} \delta(k, u) + 3 \gamma^2 \delta(k, u) = S[\delta; u] . \quad (2.85)$$

The source term is

$$S[\delta; u] = S_B[u] + S_{NB}[\delta; u] \quad (2.86)$$

where $S_B[u]$ and $S_{NB}[\delta; u]$ play the role of the Born and next to Born approximations,

$$S_B[u] = \ddot{I} + 3 \gamma^2 I \quad (2.87)$$

$$S_{NB}[\delta; u] = \int_0^u du' K(u - u') \frac{\delta(k, u')}{[1 - u']^2} . \quad (2.88)$$

As discussed above [see eq.(2.81)], in cosmic time the left hand side of eq.(2.85) is precisely of the form of the Jeans equation for fluids. The right hand side $S[\delta; u]$ may be interpreted as an additional pressure term non-local in time which includes free-streaming through the initial condition in S_B . In the long wavelength limit $S[\delta; u]$ vanishes along with the usual pressure term $3 \gamma^2 \delta(k, u)$ leading to the usual fluid-like equation for cold-dark matter density perturbations.

Eq.(2.85) lends itself to a Fredholm (iterative) solution, the basis of which is the homogeneous solution and the retarded Green's function of the differential operator on the left in eq.(2.85).

For $S[\delta, u] = 0$, eq.(2.85) becomes the homogeneous differential equation

$$\ddot{\delta}^{(0)}(k, u) - \frac{6}{(1-u)^2} \delta^{(0)}(k, u) + 3\gamma^2 \delta^{(0)}(k, u) = 0. \quad (2.89)$$

which is solved in terms of Bessel's functions. The general solution is given by

$$\delta^{(0)}(z) = A h_1(z) + B h_2(z), \quad (2.90)$$

with

$$z \equiv z_0 (1-u) \quad , \quad z_0 = \sqrt{3} \gamma, \quad (2.91)$$

$h_1(z)$ and $h_2(z)$ are related to the spherical Bessel functions $n_2(z)$ and $j_2(z)$ [49],

$$h_1(z) \equiv -z n_2(z) = \left(\frac{3}{z^2} - 1 \right) \cos z + \frac{3}{z} \sin z, \quad (2.92)$$

$$h_2(z) \equiv z j_2(z) = \left(\frac{3}{z^2} - 1 \right) \sin z - \frac{3}{z} \cos z, \quad (2.93)$$

$h_1(z)$ and $h_2(z)$ are the fundamental irregular and regular solutions, respectively, with the small argument behavior for $z \rightarrow 0$ ($u \rightarrow 1$):

$$h_1(z) \stackrel{z \rightarrow 0}{\equiv} \frac{3}{z^2}, \quad h_2(z) \stackrel{z \rightarrow 0}{\equiv} \frac{z^3}{15}, \quad (2.94)$$

and Wronskian

$$W[z] = h_2'(z) h_1(z) - h_1'(z) h_2(z) = 1, \quad (2.95)$$

where the prime denotes d/dz . The mode functions $h_{1,2}(u)$ are identified as the growing and decaying solutions of Jeans's fluid equations (2.81). The initial conditions eq.(2.48) yield

$$\delta^{(0)}(z_0) = 1 \quad , \quad \delta^{(0)'}(z_0) = 0. \quad (2.96)$$

Using eq.(2.95) we find

$$A = h_2'(z_0) \quad , \quad B = -h_1'(z_0), \quad (2.97)$$

and the homogeneous solution is given by

$$\delta^{(0)}(z) = h_2'(z_0) h_1(z) - h_1'(z_0) h_2(z). \quad (2.98)$$

Using the small argument behavior eq.(2.94), for $\gamma = 0$ ($k = 0$) the homogeneous solution $\delta^{(0)}(z)$ reduces to eq.(2.52).

The general solution: The inhomogeneous equation (2.85) can be formally solved in terms of the retarded Green's function of the differential operator on its left hand side which obeys

$$\left[\frac{d^2}{du^2} - \frac{6}{(1-u)^2} + 3\gamma^2 \right] G(u, u') = \delta(u - u'). \quad (2.99)$$

$G(u, u')$ can be explicitly written in terms of $h_{1,2}(u)$ [eqs. (2.92)-(2.93)] as,

$$G(u, u') = \frac{1}{\sqrt{3}\gamma} [h_1(u) h_2(u') - h_2(u) h_1(u')] \Theta(u - u'). \quad (2.100)$$

The formal solution of eq.(2.85) is then given by

$$\delta(k, u) = \delta^{(0)}(z) + \frac{1}{\sqrt{3}\gamma} \int_0^u [h_1(u) h_2(u') - h_2(u) h_1(u')] S[\delta; u'] du'. \quad (2.101)$$

It is convenient to separate explicitly the source term $S_B[u]$ eq.(2.87) which does not involve the kernel $K(u-u')$, but only involves the free streaming solution of the Boltzmann equation in absence of self-gravity. Integrating by parts twice the term with \ddot{I} , using the differential equation (2.99) obeyed by the Green's function and the initial conditions eq.(2.44), we obtain

$$\delta(k, u) = \delta^{(1)}(k, u) + \frac{1}{\sqrt{3}\gamma} \int_0^u [h_1(u) h_2(u') - h_2(u) h_1(u')] S_{NB}[\delta; u'] du', \quad (2.102)$$

where

$$\delta^{(1)}(k, u) = I[\alpha u] + \frac{6}{\sqrt{3}\gamma} \int_0^u [h_1(u) h_2(u') - h_2(u) h_1(u')] \frac{I[\alpha u']}{(1-u')^2} du'. \quad (2.103)$$

The gravitational potential $\Phi(k, u)$ can be analogously expressed using its relation with the density perturbation δ eq.(2.46) and eq.(2.101) with the result

$$\Phi(k, u) = \Phi^{(1)}(k, u) + \frac{1}{\sqrt{3}\gamma} (1-u)^2 \int_0^u [h_1(u) h_2(u') - h_2(u) h_1(u')] S_{NB}[\delta; u'] du', \quad (2.104)$$

where

$$\Phi^{(1)}(k, u) = (1-u)^2 \delta^{(1)}(k, u), \quad (2.105)$$

is the Born term.

It is straightforward to check that for $k=0$ the second term in eq.(2.104) vanishes and $\Phi^{(1)}(\vec{0}, u)$ is given by eq.(2.54) (for this note that $I[0]=1$).

Free streaming for $k \neq 0$ leads to collisionless Landau damping of the gravitational potential and density perturbation. Although density perturbations still grow as $1/(1-u)^2$ for $u \rightarrow 1$ the gravitational potential is bound $|\Phi| \leq 1$ and is a slow variable.

We obtain an *exact* expression for $T(k)$ inserting eqs.(2.104) into the definition of the normalized transfer function eq.(2.60) and using the small argument limits eq.(2.94),

$$T(k) = \frac{10}{\sqrt{3}\gamma^3} \int_0^1 h_2(u) \left[\frac{I[\alpha u]}{(1-u)^2} + \frac{1}{6} S_{NB}[\delta; u] \right] du, \quad (2.106)$$

where $\delta(k, u)$, argument of S_{NB} [see eq.(2.88)], is the solution of the integral equation (2.102) and we have neglected terms proportional to $a_{eq} \sim 10^{-4}$. In obtaining this result we have used the fact that $I[\alpha u]$ given by eq.(2.43) is finite at $u=1$ and that in this limit $\delta(k, u) \propto 1/(1-u)^2$. Only the terms featuring $h_1(u)$ outside the integrals survive in this limit. The terms with $h_1(u')$ inside the integrals yield at most terms $\propto 1/(1-u)^3$ but they are multiplied by $(1-u)^5$, and vanish for $u \rightarrow 1$. Furthermore, in the long wavelength limit $I[0]=1$; $S_{NB} \propto \gamma^4$ and from the small argument behavior eq.(2.94) it is straightforward to confirm that $T(k=0)=1$.

The integral equations (2.102) and (2.104) can be iterated generating the usual Fredholm series as

$$\begin{aligned} \delta(k, u) &= \delta^{(1)}(k, u) + \delta^{(2)}(k, u) + \dots, \\ \Phi(k, u) &= \Phi^{(1)}(k, u) + \Phi^{(2)}(k, u) + \dots, \end{aligned} \quad (2.107)$$

where $\delta^{(1)}(k, u)$ is given by eq.(2.103) to which we refer as the *Born* term because of its obvious similarity to the solution of a potential scattering problem,

$$\delta^{(2)}(k, u) = \frac{1}{\sqrt{3}\gamma} \int_0^u [h_1(u) h_2(u') - h_2(u) h_1(u')] S_{NB}[\delta^{(1)}; u'] du' \quad (2.108)$$

$$S_{NB}[\delta^{(1)}; u] = \int_0^u du' K(u-u') \frac{\delta^{(1)}(k, u')}{[1-u']^2}, \quad (2.109)$$

$\Phi^{(1)}(k, u)$ is given by eq.(2.105) and

$$\Phi^{(2)}(k, u) = (1-u)^2 \frac{1}{\sqrt{3}\gamma} \int_0^u [h_1(u) h_2(u') - h_2(u) h_1(u')] S_{NB}[\delta^{(1)}; u'] du'. \quad (2.110)$$

The small argument behavior eq.(2.94) makes manifest that the solution $\delta(k, u)$ indeed has the asymptotic behavior $\propto 1/(1-u)^2$ as $u \rightarrow 1$. Furthermore, since the function $I[\alpha u]$ describes the free-streaming solution of the Boltzmann equation in absence of self-gravity, the formal solution eq.(2.102) exhibits explicitly the free-streaming phenomenon.

The transfer function has also a systematic Fredholm expansion which up to second order yields

$$T(k) = \frac{10}{\sqrt{3} \gamma^3} \int_0^1 h_2(u) du \left[\frac{I[\alpha u]}{(1-u)^2} + \frac{1}{6} S_{NB}[\delta^{(1)}; u] \right] \equiv T_B(k) + T_{NB}(k), \quad (2.111)$$

where we refer to the first order term

$$T_B(k) = \frac{10}{\sqrt{3} \gamma^3} \int_0^1 h_2(u) du \frac{I[\alpha u]}{(1-u)^2}, \quad (2.112)$$

as the *Born* term because its origin is the Born term for the gravitational potential $\Phi^{(1)}(k, u)$ and

$$T_{NB}(k) = \frac{5}{3\sqrt{3} \gamma^3} \int_0^1 h_2(u) S_{NB}[\delta^{(1)}; u] du, \quad (2.113)$$

is the next to Born (second order) correction, where $\delta^{(1)}(k; u)$ and $S_{NB}[\delta^{(1)}; u]$ are given by eqs.(2.103) and (2.109), respectively.

At this point it is worthwhile to emphasize the following important aspect: the first order, Born term in the transfer function only depends on the initial condition and describes the free-streaming suppression. The second order term, the integral of S_{NB} , contains the information on the higher moments of the *distribution function* of the decoupled particles and the corrections to the fluid approximation through the non-local kernel $K(u-u')$ eq.(2.76). The details of the distribution function beyond the first moment $\langle \vec{p}^2 \rangle$ enter the transfer function at second order and beyond in the Fredholm series. It will be shown below that these contributions include *memory of gravitational clustering* and become important at short wavelengths $\gamma > 1$.

Eq.(2.111) provides a useful approximation to the transfer function for general initial conditions and distribution functions. Specific examples for which we obtain an exact numerical evaluation (see below) show that the second order approximation eq.(2.111) is *remarkably accurate* in a wide range of scales. These are some of the main results of this article.

III. COLD DARK MATTER: NON-RELATIVISTIC, MAXWELL-BOLTZMANN DISTRIBUTION.

The unperturbed distribution function for particles that decoupled while non-relativistic in local thermal equilibrium is a solution of the collisionless Boltzmann-equation (in absence of gravitational perturbations), given by

$$f_0(P_f(t), t) = \mathcal{N} e^{-\frac{P_f^2(t) a^2(t)}{2m T_d a_d^2}}, \quad (3.1)$$

where the explicit expression for the normalization factor \mathcal{N} may be found in ref.[39], $P_f(t)$ is the physical momentum, $a(t)$ is the scale factor and T_d , a_d are the temperature and scale factor at decoupling respectively. Since $p = P_f(t) a(t)$ is the comoving momentum (equal to the physical momentum *today*) and $T_d a_d = T_{d,0}$ is the decoupling temperature *today*, the unperturbed Maxwell-Boltzmann distribution function can be written in terms of dimensionless variables as

$$f_0(y; x) = \mathcal{N} e^{-\frac{y^2}{2x}}, \quad y = \frac{p}{T_{d,0}}, \quad x = \frac{m}{T_d}, \quad (3.2)$$

and the normalized distribution function is given by

$$\tilde{f}_0(y) = \frac{4}{\sqrt{\pi} [2x]^{\frac{3}{2}}} e^{-\frac{y^2}{2x}}, \quad (3.3)$$

$\overline{y^2}$ [eq.(2.72)] and α [eq.(2.73)] are in this case,

$$\overline{y^2} = 3 \frac{m}{T_d}, \quad \alpha = \sqrt{\frac{T_d}{m}} \gamma. \quad (3.4)$$

The typical values of the masses and decoupling temperatures for WIMPs are $m \sim 100$ GeV and $T_d \sim 10$ MeV [48], for which $g_d \sim 10$ [2]. Using the result for the free-streaming wavevector today eq.(2.79) we find

$$k_{fs}(t_{eq}) = \frac{5.88}{\text{pc}} \left(\frac{g_d}{2} \right)^{\frac{1}{3}} \left(\frac{m}{100 \text{ GeV}} \right)^{\frac{1}{2}} \left(\frac{T_d}{10 \text{ MeV}} \right)^{\frac{1}{2}}. \quad (3.5)$$

Within the cosmologically relevant range of scales where the linearized approximation is valid, eq.(2.39) and using (2.73) it follows that in this range $\gamma \leq 10^{-5}$.

The kernel $\Pi[\alpha(u-u')]$ that enters in the Volterra equation (2.47) is best obtained by performing the momentum integrals of the distribution function in cartesian coordinates rather than performing the angular integration first. This is a consequence of the fact that the distribution function is a function of \vec{p}^2 . We obtain the following equation for density perturbations

$$\delta(k, u) - 6 \int_0^u du' (u-u') e^{-\frac{\gamma^2}{2}(u-u')^2} \frac{\delta(k, u')}{[1-u']^2} = I[\gamma u], \quad (3.6)$$

where $I[\gamma u]$ [eq.(2.43)] is the inhomogeneity determined by the initial condition. Taking two derivatives with respect to u and using eq.(3.6) we obtain

$$\ddot{\delta}(k, u) - \frac{6}{1-u^2} \delta(k, u) + 3\gamma^2 \delta(k, u) - 6\gamma^4 \int_0^u du' (u-u')^3 e^{-\frac{\gamma^2}{2}(u-u')^2} \frac{\delta(k, u')}{[1-u']^2} = \ddot{I}[\gamma u] + 3\gamma^2 I[\gamma u]. \quad (3.7)$$

From this expression we obtain the explicit form of the kernel $K(u-u')$ that defines the source term eq.(2.88) and enters in the transfer function eq.(2.106), namely

$$K(u-u') = 6\gamma^4 (u-u')^3 e^{-\frac{\gamma^2}{2}(u-u')^2}. \quad (3.8)$$

In the cosmologically relevant case $\gamma \leq 10^{-5}$, we can safely approximate the density perturbation, gravitational potential and transfer function by their Born term in the Fredholm series, namely

$$\delta^{(1)}(k, u) = I[\gamma u] + \frac{6}{\sqrt{3}\gamma} \int_0^u [h_1(u) h_2(u') - h_2(u) h_1(u')] \frac{I[\gamma u']}{(1-u')^2} du', \quad (3.9)$$

$$\Phi^{(1)}(k, u) = (1-u)^2 \delta^{(1)}(k, u), \quad (3.10)$$

$$T_B(k) = \frac{10}{\sqrt{3}\gamma^3} \int_0^1 h_2(u) \frac{I[\gamma u]}{(1-u)^2} du. \quad (3.11)$$

For the sake of comparison with the exact result and to display the dependence on initial conditions we study both initial conditions eqs.(2.65) and (2.66). The calculation of $I[\gamma u]$ in both cases is best performed with cartesian coordinates, we find for the case of temperature perturbations eq.(2.65)

$$I_T[\gamma u] = \left[1 - \frac{1}{3} \gamma^2 u^2 \right] e^{-\frac{1}{2} \gamma^2 u^2}, \quad (3.12)$$

and for Gilbert's initial condition eq.(2.66)

$$I_G[\gamma u] = e^{-\frac{1}{2} \gamma^2 u^2}. \quad (3.13)$$

They are connected by the simple relationship

$$I_T[\gamma u] = \left(1 + \frac{1}{3} \gamma \frac{\partial}{\partial \gamma} \right) I_G[\gamma u]. \quad (3.14)$$

Figs. 1 and 2 display the exact results for $\Phi(k; u)$ and $T^2(k)$ obtained by numerical integration of eq.(3.6) and using the relation (2.46), compared to the solution obtained with the Born approximation. It is clear that the Born approximation is remarkably accurate for $\gamma \lesssim 1$, namely $k \lesssim k_{fs}(t_{eq})$. Fig. 3 compares $T^2(k)$ for the initial conditions eq.(3.13) and eq.(3.12). The exact numerical results are indistinguishable from the Born approximation in the range displayed.

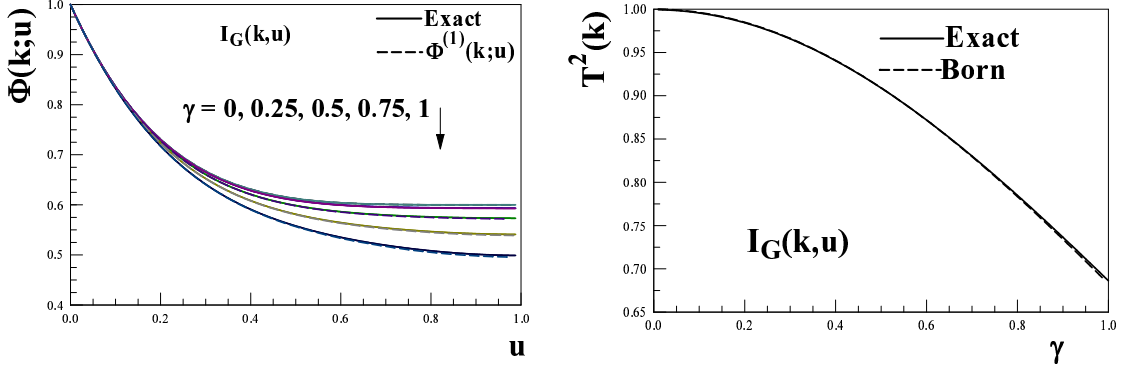


FIG. 1: Non-relativistic, Maxwell-Boltzmann distribution. Left panel: The gravitational potential $\Phi(k, u)$ vs. u for $\gamma = 0, 0.25, 0.4, 0.75, 1$. Right panel: the transfer function $T^2(k)$ vs. γ . In both cases the solid line corresponds to the exact solution of eq. (2.47) with the initial condition eq.(3.13) and the dashed line to the Born approximation eqs.(3.10) and (3.11).

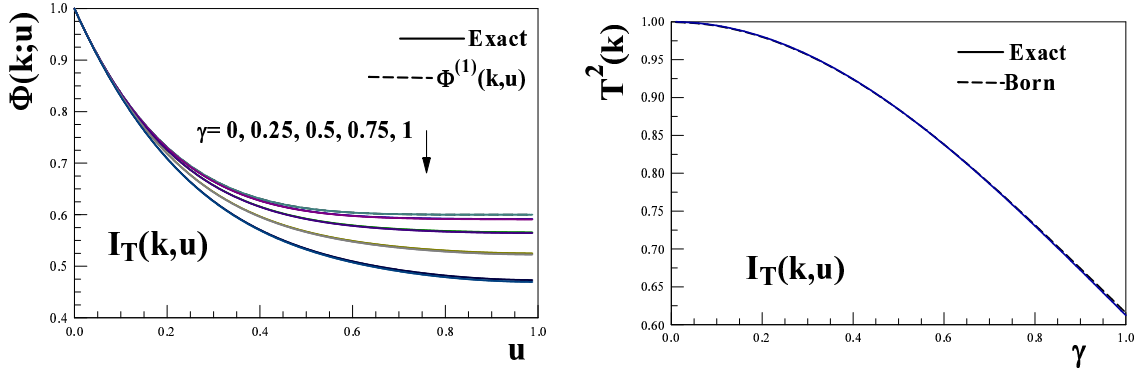


FIG. 2: Non-relativistic, Maxwell-Boltzmann distribution. Left panel: $\Phi(k, u)$ vs γ for $\gamma = 0, 0.25, 0.4, 0.75, 1$. Right panel: $T^2(k)$ vs. γ . In both cases the solid line corresponds to the exact solution of eq. (2.47) with the initial condition eq.(3.12) and the dashed line to the the Born approximation eqs.(3.10) and (3.11).

A. Short wavelength: memory of gravitational clustering

Although for WIMPs only the region of $\gamma \ll 1$ is of cosmological relevance as discussed above, it is important to study the opposite limit $\gamma \gg 1$ to understand how the memory kernel $K(u - u')$ modifies the transfer function. It proves convenient to change variables to $z = \gamma(u - u')$ and to replace in eq.(2.88) the density perturbation δ by the gravitational potential $\Phi(k, u)$ which is bounded in time, to write

$$S_{NB}(u) = 6 \int_0^{\gamma u} z^3 e^{-\frac{z^2}{2}} \frac{\Phi[k; u - \frac{z}{\gamma}]}{[1 - u + \frac{z}{\gamma}]^4} dz \quad (3.15)$$

Since $\Phi(k; u \sim 0) \sim 1$ it is clear from this expression that S_{NB} is negligible either at small time ($u \ll 1/\gamma$) or in the long wavelength limit $\gamma \ll 1$. The factor $z^3 e^{-\frac{z^2}{2}}$ in the integrand grows as z^3 at small z , attains a maximum at $z = \sqrt{3}$, namely $u - u' \sim 1/\gamma$, and falls-off exponentially for $z > \sqrt{3}$ for $1 - u \gg 1/\gamma$.

Therefore, S_{NB} begins to contribute for $u > 1/\gamma$. Since $\Phi(k, u)$ is still $\sim \mathcal{O}(1)$ during this interval it follows that S_{NB} becomes of $\mathcal{O}(1)$, whereas for large γ the Born term for Gilbert's initial conditions,

$$S_{B,G} = \gamma^2 [2 + \gamma^2 u^2] e^{-\frac{1}{2} \gamma^2 u^2}, \quad (3.16)$$

is suppressed for $u \gg 1/\gamma$. Analogous conclusions follow for temperature perturbations where the expression for $S_{B,A}$ follows combining eqs.(3.14) and (3.16).

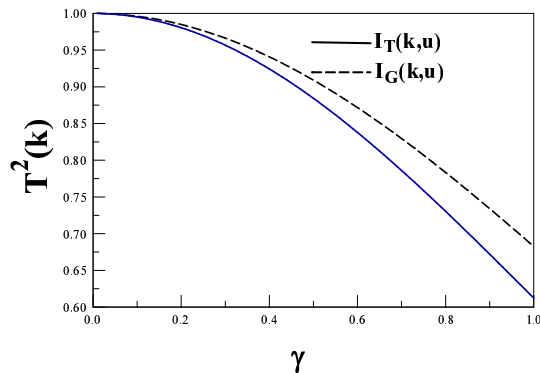


FIG. 3: Non-relativistic, Maxwell-Boltzmann distribution. Comparison between $T^2(k)$ vs. γ for the initial conditions eqs.(3.12) and (3.13). The exact result and the Born approximation are indistinguishable in this range.

Therefore, for $\gamma \gg 1$ there is a crossover in behavior: during $0 \leq u \leq 1/\gamma$ the Born term which dominates is of $\mathcal{O}(1)$ and the second order correction is negligible, while at $u \sim 1/\gamma$ both terms become of the same order, and for $u > 1/\gamma$ the second order correction becomes important. Finally, for $1 - u \ll 1/\gamma$ the small z region dominates yielding a logarithmic behavior for the second order correction. When this correction becomes important for $\gamma \gg 1$, the transfer function $T(k)$ is very small, suppressed at least by the prefactor $1/\gamma^3$.

For $\gamma \gg 1$, in the region with $\gamma u \gg 1$ the upper limit of the integral can be taken to infinity. For $1/\gamma \ll u \ll 1 - 1/\gamma$ the dominant contribution arises from the region $u \sim 0$ where $\Phi \sim 1$ is largest, in this region the full integral is of $\mathcal{O}(1)$.

Furthermore, since to leading order Φ decays via free-streaming on a time scale $u \sim 1/\gamma$, its derivative is large during the initial free-streaming regime but becomes small for $u \geq 1/\gamma$ as can be gleaned from Figs 1-2. This analysis leads to the conclusion that $S_{NB}(u)$ becomes important for $\gamma \gg 1$ in the region $\gamma u \gg 1$, where it is of the same order (or larger) than the free streaming contribution (Born term). When $S_{NB}(u)$ becomes non-negligible the transfer function is suppressed by $\sim 1/\gamma^3$. Therefore, the corrections to the Born term become relevant at small scales when the transfer function has diminished substantially.

In the region $u \gg 1/\gamma$ the following *Markovian* approximation is reliable:

$$\Phi[k; u - \frac{z}{\gamma}] \approx \Phi[k; u] - \dot{\Phi}[k; u] \frac{z}{\gamma} + \dots \quad (3.17)$$

We emphasize that this Markovian approximation is valid only after the initial free streaming transient for $u > 1/\gamma$, since during the transient $\dot{\Phi} \sim \gamma$. Therefore, although such Markovian approximation is available after the initial transient, the value of the gravitational potential must be *matched* to that at the end of the free-streaming period in order to provide the full dynamical evolution.

The analysis above suggests that the influence of the memory kernel $K(u - u')$ becomes important for short wavelengths $\gamma > 1$. Thus, for scales $\lambda \leq \lambda_{fs}(t_{eq}) \sim l_{fs}(v; 0)$ where $\gamma > 1$ we need to include the *second order* term in the Fredholm expansion in the transfer function given by eq.(2.111), where

$$S_{NB}[\delta^{(1)}; u] = 6 \gamma^4 \int_0^u du' (u - u')^3 e^{-\frac{\gamma^2}{2} (u - u')^2} \frac{\delta^{(1)}(k, u')}{[1 - u']^2} \quad (3.18)$$

and $\delta^{(1)}(k, u)$ is given by eq.(3.9). Higher order terms are further suppressed by extra powers of $1/\gamma$ in the transfer function.

The addition of the second order correction yields a *remarkably accurate* fit to the exact solution of the Boltzmann-Vlasov equation in a wide range of scales down to scales $\lambda \ll \lambda_{fs}(t_{eq})$.

Fig. 4 displays the comparison between the exact result for $T^2(k)$ compared with both the Born approximation and the next to Born approximation for initial conditions eq.(3.13). Fig. 5 displays the same comparison for the initial condition eq.(3.12). These figures confirm the analysis presented above: the Born term is a fairly accurate approximation in the region $\gamma \lesssim 1$ and the second order correction becomes significant at $\gamma \sim 1$. Including the second order correction yields a remarkably accurate approximation in a wide range of scales $0 < \gamma < 5$.

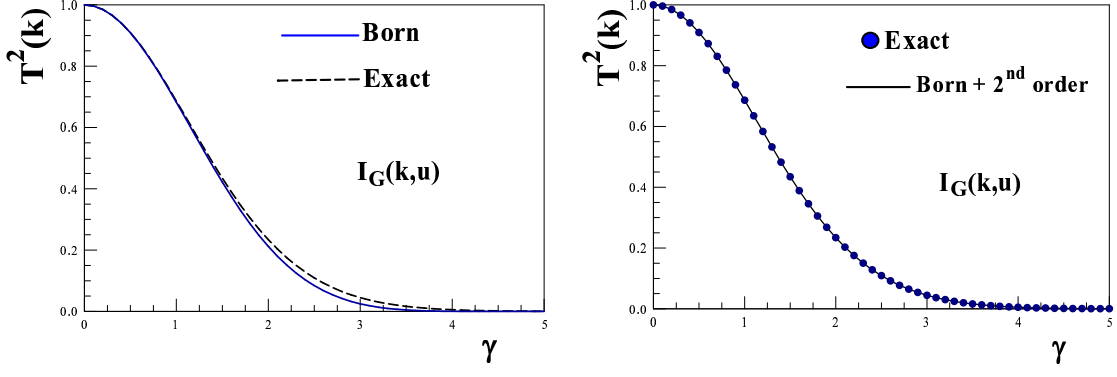


FIG. 4: Non-relativistic, Maxwell-Boltzmann distribution. Left panel: The transfer function $T^2(k)$ vs. γ for the exact solution and the Born approximation. Right panel: $T^2(k)$ vs. γ for the exact solution and the Born approximation plus second order. Gilbert's initial condition eq.(3.13) was used.

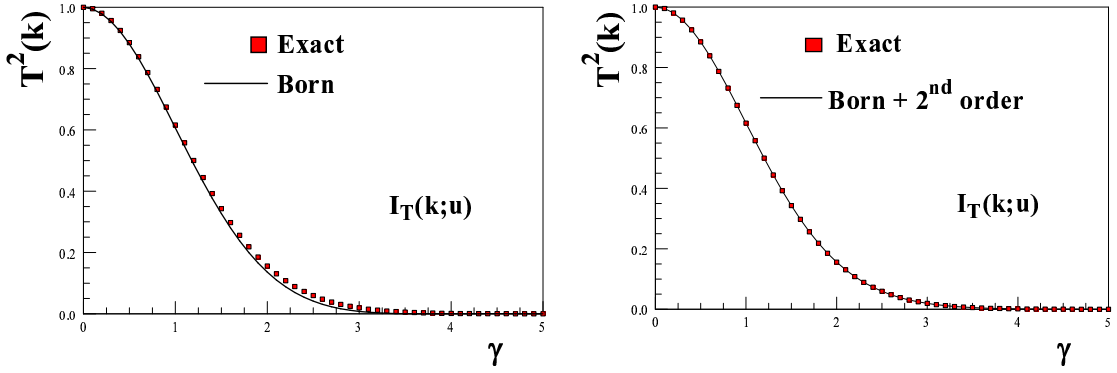


FIG. 5: Non-relativistic, Maxwell-Boltzmann distribution. Left panel: the transfer function $T^2(k)$ vs γ for the exact solution and the Born approximation. Right panel: $T^2(k)$ vs. γ for the exact solution and the Born approximation plus second order. Initial condition for temperature fluctuations eq.(2.65)

We obtain $T(k)$ for large scales expanding eq.(3.13) for small γu

$$I_G[\gamma u] \stackrel{\gamma u \rightarrow 0}{\approx} 1 - \frac{1}{2} \gamma^2 u^2 + \mathcal{O}(\gamma^4 u^4), \quad (3.19)$$

and follow the same steps leading to eq.(2.69), setting $b = 1/2$ according to eqs.(2.63) and (3.19), and replacing α by γ in eq.(2.69), with the result

$$T(k) = 1 - \left(\frac{\gamma}{\gamma_0}\right)^2 + \mathcal{O}(\gamma^4) \quad (3.20)$$

where

$$\gamma_0 = \begin{cases} \sqrt{\frac{21}{8}} = 1.62 \dots & \text{Gilbert initial conditions,} \\ \sqrt{\frac{126}{62}} = 1.42 \dots & \text{Temperature initial conditions.} \end{cases} \quad (3.21)$$

γ_0 characterizes the fall-off of $T(k)$. We find for a given initial condition γ_0 is independent of the statistics for thermal relics.

For WIMPs the long-wavelength approximation (3.20) describes $T(k)$ in the whole range of scales of cosmological relevance for structure formation in the linear regime, since for these scales $\gamma \lesssim 10^{-5}$ and the Born approximation describes the DM density and gravitational perturbations outstandingly well.

Although for the scales of interest for structure formation $T(k)$ given by (3.20) gives the correct description, it is illuminating to study the small scale behavior of $T(k)$.

The precise numerical solution of eq.(3.6) shows that $T(k)$ for temperature initial conditions has a zero at $\gamma = 7.7\dots$ as shown in fig. 10 and is negative for $\gamma > 7.7\dots$ decreasing exponentially for $\gamma > 10$ as

$$|T(k)| \simeq e^{-\left(\frac{\gamma}{\gamma_{MB}}\right)^{x_{MB}}} \quad (3.22)$$

where $x_{MB} \simeq 1.3$ and $\gamma_{MB} \simeq 1.55$ both for temperature and Gilbert initial conditions eqs.(2.65) and (2.66).

We draw the following important lessons from this study:

- For $k \leq k_{fs}(t_{eq})$, the Born approximation gives a simple and very accurate description of the transfer function. It inputs the free streaming solution in absence of self-gravity and the mode functions associated with the fluid description. These *only* input the average squared velocity, therefore the first moment $\langle p^2 \rangle$ of the distribution function. This approximate but fairly accurate solution yields a simple tool to understand different distribution functions and initial conditions in generic situations.
- The short wavelength region of the transfer function $k > k_{fs}(t_{eq})$ is remarkably well described by correcting the Born approximation with the second order term in the Fredholm solution. This correction incorporates higher moments of the distribution function and includes important *memory effects* of gravitational clustering and corrections to the fluid description. This approximation while just slightly more involved than the Born term also yields a rather simple and systematic tool to study the effects of *higher order correlations* and the full structure of the distribution function along with memory of gravitational clustering in generic situations.
- We see that the scale characterizing the suppression of $T(k)$ with γ **decreases** with k (and γ). Namely, γ_0 characterizing the suppression for small k is larger than the characteristic suppression scale for larger k .

Nevertheless, the numerical study shows that the characteristic suppression scale k_{char} related to a characteristic dimensionless ratio γ_{char} by eqs.(2.33), (2.36), (2.38) and (3.4), namely:

$$k_{char} = \frac{1}{2} H_0 \sqrt{\Omega_M a_{eq}} \left(\frac{g_d}{2}\right)^{\frac{1}{3}} \frac{\sqrt{T_d m}}{T_{cmb}} \gamma_{char} = 4.17 \left(\frac{g_d}{2}\right)^{\frac{1}{3}} \left(\frac{m}{100 \text{ GeV}}\right)^{\frac{1}{2}} \left(\frac{T_d}{10 \text{ MeV}}\right)^{\frac{1}{2}} \frac{\gamma_{char}}{\text{pc}}. \quad (3.23)$$

is such that in all cases considered we find $\gamma_{char} \sim \mathcal{O}(1)$. Therefore, $k_{fs}(t_{eq})$ obtained from free particle propagation [eqs.(2.26)-(2.27)] and given by equations (2.79,3.5) only differs by a factor of order one from k_{char} [eq.(3.23)].

IV. WARM AND HOT DARK MATTER: FERMIONS VS. BOSONS

In this section we consider thermal relics that decoupled in LTE while ultrarelativistic, but that have become non-relativistic during matter domination. Their normalized distribution function after freeze-out are given by

$$\tilde{f}_0(y) = \frac{2}{3 \zeta(3)} \frac{1}{e^y + 1} \quad \text{FD}, \quad (4.1)$$

$$\tilde{f}_0(y) = \frac{1}{2 \zeta(3)} \frac{1}{e^y - 1} \quad \text{BE}, \quad y = \frac{p}{T_{d,0}}, \quad (4.2)$$

for FD and BE respectively, with $T_{d,0}$ being the decoupling temperature today. We study each case separately.

It is convenient to state the following general result in order to estimate the large momentum contribution of the various integrals. Consider a generic integral of the form

$$\int_0^\infty F(y) \sin[yz] dy, \quad (4.3)$$

where $F(0)$, $F'(0)$, $F''(0)\dots$ are finite and $F(\infty) = 0$. Integrating by parts consecutively we find the large z behavior

$$\int_0^\infty F(y) \sin[yz] dy = \frac{F[0]}{z} - \frac{F''[0]}{z^3} + \mathcal{O}\left(\frac{1}{z^5}\right). \quad (4.4)$$

This result will be useful in the analysis that follows.

$T(k)$ decreases in k with a characteristic scale k_{char} which depends on the initial conditions, the particle statistics and the regime of wavenumbers. k_{char} translates into a characteristic scale α_{char} in the dimensionless variable α . k_{char} is related to α_{char} by eqs.(2.33), (2.36) and (2.38):

$$k_{char} = \frac{1}{2} H_0 \sqrt{\Omega_M a_{eq}} \left(\frac{g_d}{2}\right)^{\frac{1}{3}} \frac{m}{T_{cmb}} \alpha_{char} = 0.00417 \alpha_{char} \left(\frac{g_d}{2}\right)^{\frac{1}{3}} \frac{m}{\text{keV}} [\text{kpc}]^{-1}. \quad (4.5)$$

For fermionic and bosonic thermal relics $\alpha_{char} \sim \text{O}(1)$ because in these cases $\overline{y^2} \sim \text{O}(1)$.

A. Fermions

For fermions that decoupled relativistically in LTE with the normalized distribution function eq.(4.1), it follows that

$$\overline{y^2} = \int_0^\infty y^4 \tilde{f}_0(y) dy = 15 \frac{\zeta(5)}{\zeta(3)} = 12.939 \dots, \quad (4.6)$$

leading from eq.(2.79) to the free-streaming wavevector today

$$k_{fs}(t_{eq}) = 0.00284 \dots \left(\frac{g_d}{2}\right)^{\frac{1}{3}} \frac{m}{\text{keV}} [\text{kpc}]^{-1}. \quad (4.7)$$

For the initial condition eq.(2.65) the inhomogeneity is

$$I_T[\alpha u] = \frac{2}{9 \zeta(3)} \int_0^\infty \frac{y^2 e^y}{(e^y + 1)^2} \frac{\sin[y \alpha u]}{\alpha u} dy = \frac{4}{3 \zeta(3)} \sum_{n=1}^\infty \frac{(-1)^{n+1} n}{(n^2 + z^2)^2} \left[1 - \frac{4}{3} \frac{z^2}{(n^2 + z^2)}\right], \quad z = \alpha u, \quad (4.8)$$

whereas for the initial condition eq.(2.66)

$$I_G[\alpha u] = \frac{2}{3 \zeta(3)} \int_0^\infty \frac{y}{e^y + 1} \frac{\sin[y \alpha u]}{\alpha u} dy = \frac{4}{3 \zeta(3)} \sum_{n=1}^\infty \frac{(-1)^{n+1} n}{(n^2 + z^2)^2}, \quad z = \alpha u. \quad (4.9)$$

Using the result eq.(4.4) we find that for both initial conditions the asymptotic behavior of the inhomogeneity for $\alpha u \gg 1$ is given by

$$I_G[\alpha u] \stackrel{\alpha u \rightarrow \infty}{\sim} \frac{1}{3 \zeta(3) (\alpha u)^4} + \mathcal{O}\left(\frac{1}{[\alpha u]^6}\right), \quad I_T[\alpha u] \stackrel{\alpha u \rightarrow \infty}{\sim} -\frac{1}{9 \zeta(3) (\alpha u)^4} + \mathcal{O}\left(\frac{1}{[\alpha u]^6}\right), \quad (4.10)$$

which must be contrasted to the Maxwell-Boltzmann case for which $I_G[\alpha u]$ and $I_T[\alpha u]$ eqs.(3.12) and (3.13) decay exponentially.

Therefore, FD statistics results in free-streaming solutions in absence of self-gravity $I_G[\alpha u]$ and $I_T[\alpha u]$ that fall off much slower, with a power law in time. Such long-range feature is also present in the kernel $K(u - u')$. This is unlike the Maxwell-Boltzmann case where such free-streaming solutions eqs.(3.12) and (3.13) fall-off exponentially on a time scale $1/\gamma$.

Implementing the result eq.(4.4) we find that the kernel $K(u - u')$ eq.(2.76) with the normalized FD distribution function eq.(4.1) falls off as

$$K(u - u') \stackrel{(u-u') \rightarrow \infty}{\sim} \frac{30 \zeta(5)}{\zeta^2(3)} \frac{\alpha}{[\alpha (u - u')]^3} \text{ FD} \quad (4.11)$$

Fig. 6 displays both $K[z]/[6 \alpha]$ and $z^3 K[z]/[6 \alpha]$. Again this case must be contrasted with the Maxwell-Boltzmann case eq.(3.8) which decays exponentially.

Thus, whereas for $\gamma \gg 1$ the Maxwell-Boltzmann distribution leads to a short range memory kernel, the FD distribution yields a long range kernel that keeps memory of the initial state and the initial value of the gravitational and density perturbations.

For the FD case eqs.(2.73) and (4.6) yield

$$\alpha = \sqrt{\frac{\zeta(3)}{5 \zeta(5)}} \gamma = 0.482 \dots \gamma. \quad (4.12)$$

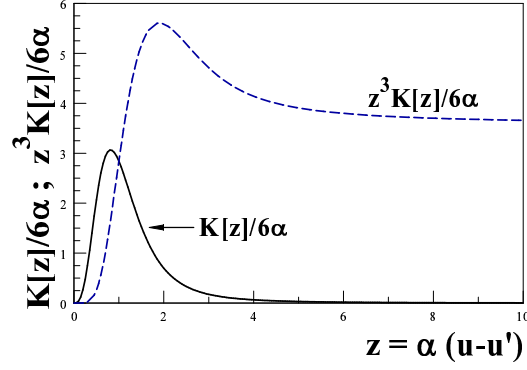


FIG. 6: The kernel $K(u - u')/[6\alpha]$ [see eq.(2.76)] vs. $z = \alpha(u - u')$ for Fermionic thermal relics.

We can now study the transfer function as a function of γ comparing the exact result with the Born approximation eq.(2.112) and the next to Born term eq.(2.113). The analysis presented in the previous section of the different contributions also applies to this case:

For long wavelengths $\gamma < 1$ the second order correction $S[\delta^1, u]$ is much smaller than the Born term because the kernel $K(u - u')$ is of order γ^4 , hence $T(k)$ is dominated by the Born term and by the free streaming solution.

At shorter wavelengths $\gamma > 1$ the kernel $K(u - u')$ begins to contribute at $u > 1/\gamma$ and peaks at $u' \sim u$ as indicated by Fig. 6 but by this time both the density perturbation and gravitational potential inside the integrand have decayed substantially leading to a suppressed contribution to the transfer function.

This analysis leads to conclude that for $\gamma < 1$, $T(k)$ is dominated by the Born term while second (and higher) order corrections become relevant for $\gamma > 1$.

We have confirmed this analysis by comparing the exact numerical solution of Gilbert's equation with the Born approximation and the second order correction to the transfer function for both initial conditions eqs.(4.8) and (4.9). The results are qualitatively the same in both cases and we present them for temperature initial conditions in fig. 7. The agreement between the exact result and the Born plus second order correction is remarkable. The numerical study confirms the analysis above, the second order contribution, which includes the memory of gravitational clustering becomes important for $\gamma > 1$, namely at small scales, but when it begins to be appreciable, $T(k)$ has been highly suppressed. For $\gamma \gtrsim 5$ we find that $T^2(k) \lesssim 10^{-5}$.

$T(k)$ for large scales follows from eq.(2.69) and

$$I_G[\alpha u] \stackrel{\alpha u \rightarrow 0}{\approx} 1 - \frac{5}{2} \frac{\zeta(5)}{\zeta(3)} (\alpha u)^2 + \mathcal{O}([\alpha u]^4) ,$$

for fermions. We find that the large scale approximation for $T(k)$ eq.(3.20) is **also valid** in the FD case.

The precise numerical resolution of eq.(3.6) for fermions shows that $T(k)$ for Gilbert initial conditions [eq.(2.66)] and $\gamma > 4$ decreases as

$$T(k) \simeq \left(\frac{\gamma_{fg}}{\gamma} \right)^{x_{fg}} , \quad x_{fg} \simeq 7.6 \quad , \quad \gamma_{fg} \simeq 3.7 , \quad (4.13)$$

see fig. 10.

The behavior of $T(k)$ for temperature initial conditions [eq.(2.65)] is more involved as displayed in fig. 10: we find that $T(k)$ decreases exponentially for $4 < \gamma < 15$ as

$$T(k) \simeq c_{fa} e^{-\frac{\gamma}{\gamma_{fa1}}} , \quad c_{fa} \sim 7.6 \quad , \quad \gamma_{fa1} \simeq 0.89 . \quad (4.14)$$

For $\gamma > 15$ $T(k)$ decreases faster than in eq.(4.14), it vanishes and becomes negative at $\gamma \simeq 16.72$. For $\gamma > 25$ $T(k)$ decreases in absolute value as power law:

$$T(k) \simeq - \left(\frac{\gamma_{fa2}}{\gamma} \right)^{x_{fa}} , \quad x_{fa} \simeq 5.3 \quad , \quad \gamma_{fa2} \simeq 0.96 . \quad (4.15)$$

We find that the scale of suppression itself slides with scale.

For Gilbert initial conditions, we see that the characteristic fall-off scale of $T(k)$ **increases** with increasing k , from $\gamma_0 \simeq 1.62 \dots$ for small k to $\gamma_{fg} \simeq 3.7$ for $\gamma > 6$. Instead, for temperature initial conditions, the characteristic fall-off scale **decreases** with increasing k reaching values $\gamma_{fa} \simeq 0.89 - 0.96$ for $\gamma > 4$. However, all of these are of the same order $\sim \mathcal{O}(1)$ which is a manifestation of a *unique characteristic* scale $\gamma_{char} \sim \mathcal{O}(1)$ as also found in the case of the Maxwell-Boltzmann distribution.

Therefore, in terms of wavevector k this observation translates into the statement that the relevant scale for suppression of $T(k)$ is $k_{fs}(t_{eq})$, although the functional form of $T(k)$ itself depends on scale and initial condition, in this case varying from exponential to power law.

We anticipate that the power law behavior of the kernel $K(u - u')$ for fermions [eq.(4.11)] leads to a longer memory on the initial conditions than in the Maxwell-Boltzmann case eq.(3.8). For $\gamma \gg 1$ the range of the Born term and that of the kernel are much longer for fermions than for the Maxwell-Boltzmann case. Then, both the free streaming solution and the gravitational perturbation (or alternatively the density perturbation) for *small* values of u' inside the integrand in $K(u - u')$ yield larger contributions for FD than for Maxwell-Boltzmann. We indeed find that $|T(k)|$ for thermal Fermions and for a given value of γ is *enhanced* relative to that of the Maxwell-Boltzmann particles [see fig. 10].

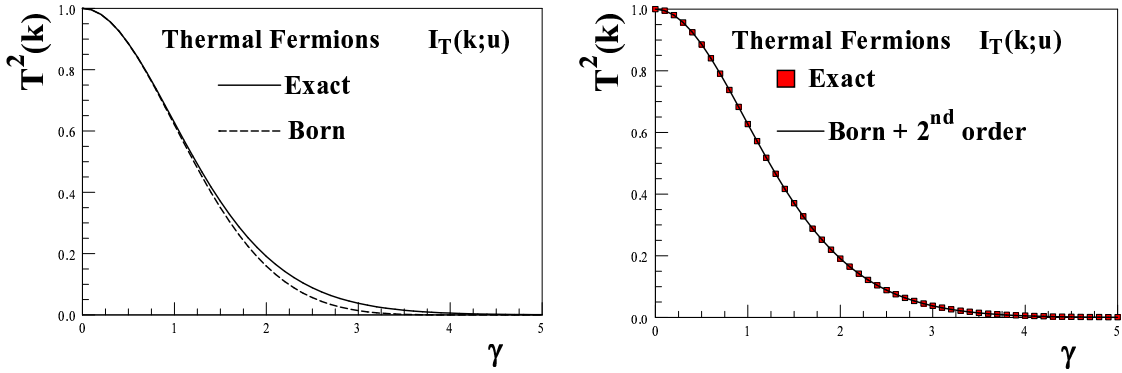


FIG. 7: Fermionic thermal relics. Left panel: $T^2(k)$ vs γ for the exact solution and the Born approximation. Right panel: $T^2(k)$ vs γ for the exact solution and the Born approximation plus second order. Initial condition given by eq.(4.8). Similar agreement is found with the initial Gilbert's conditions eq.(4.9).

B. Bosons

For thermal bosons that decoupled while relativistic with the normalized distribution function eq.(4.2) we find

$$\overline{y^2} = 12 \frac{\zeta(5)}{\zeta(3)} = 10.352 \dots \quad (4.16)$$

leading from eq.(2.79) to the free streaming wave vector today

$$k_{fs}(t_{eq}) = 0.00317 \dots \left(\frac{g_d}{2}\right)^{\frac{1}{3}} \frac{m}{\text{keV}} [\text{kpc}]^{-1}. \quad (4.17)$$

For the initial condition eq.(2.65) the inhomogeneity is

$$I_T[\alpha u] = \frac{1}{6 \zeta(3)} \int_0^\infty \frac{y^2 e^y}{(e^y + 1)^2} \frac{\sin[y \alpha u]}{\alpha u} dy = \frac{1}{\zeta(3)} \sum_{n=1}^\infty \frac{n}{(n^2 + z^2)^2} \left[1 - \frac{4}{3} \frac{z^2}{(n^2 + z^2)}\right], \quad z = \alpha u \quad (4.18)$$

and for the initial condition eq.(2.66)

$$I_G[\alpha u] = \frac{1}{2 \zeta(3)} \int_0^\infty \frac{y}{e^y + 1} \frac{\sin[y \alpha u]}{\alpha u} dy = \frac{1}{\zeta(3)} \sum_{n=1}^\infty \frac{n}{(n^2 + z^2)^2}, \quad z = \alpha u. \quad (4.19)$$

Using the result eq.(4.4) we find that the asymptotic behavior of the inhomogeneity for $\alpha u \gg 1$ for both initial conditions is given by

$$I_G[\alpha u] \stackrel{\alpha u \rightarrow \infty}{\sim} \frac{1}{2 \zeta(3) (\alpha u)^2} + \mathcal{O}\left(\frac{1}{[\alpha u]^4}\right) , \quad I_T[\alpha u] \stackrel{\alpha u \rightarrow \infty}{\sim} -\frac{1}{6 \zeta(3) (\alpha u)^2} + \mathcal{O}\left(\frac{1}{[\alpha u]^4}\right) . \quad (4.20)$$

This is an even slower power law fall off than in the FD case and even much slower than the Gaussian-exponential fall off in the Maxwell-Boltzmann case.

Since $I[\alpha u]$ is the free streaming solution in absence of self-gravity (normalized to one at the initial time), we see that with either initial condition the Bose-Einstein distribution function leads to a much less efficient free-streaming smoothing of the initial perturbation.

This long range feature associated with the Bose-Einstein distribution is also manifest in the kernel $K(u - u')$. Again, using eq.(4.4) we find that the kernel $K(u - u')$ eq. (2.76) with the normalized Bose-Einstein distribution eq.(4.2) falls off as

$$K(u - u') \stackrel{\alpha(u-u') \rightarrow \infty}{\sim} \frac{36 \zeta(5)}{\zeta^2(3)} \frac{1}{u - u'} \quad \text{BE} . \quad (4.21)$$

Fig. 8 displays both $K[z]/(6\alpha)$ and $z K[z]/(6\alpha)$. This fall-off is even slower than in the FD and certainly much slower than the Maxwell-Boltzmann case eq.(3.8), with important consequences explored below.

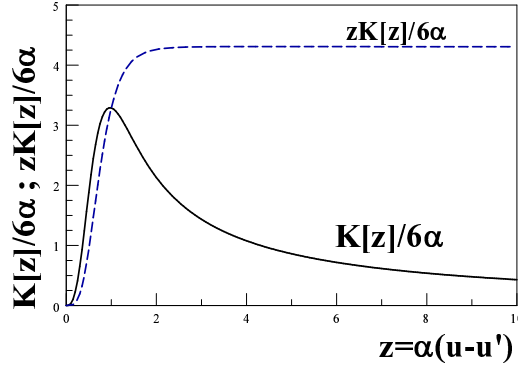


FIG. 8: The kernel $K(u - u')/[6\alpha]$ (full line) [see eq.(2.76)] and $z K[z]/(6\alpha)$ (dashed line) vs. $z = \alpha(u - u')$ for Bosonic thermal relics.

BE statistics, more specifically the behavior of the distribution function at small momentum, leads to a slow fall off with a power law and *long range memory*, even much longer than the FD case because of the divergence of the distribution function as $y \rightarrow 0$.

The long-range nature of the kernel brings about important consequences: even for $u \sim 1$ the kernel is sensitive to the region $u' \sim 0$, therefore the initial value of the gravitational potential $\Phi(k, u \sim 0) \sim 1$, which is the largest value that Φ attains, contributes with a large measure to the integrand. This feature in turn results in that free-streaming is less efficient, and a large memory of the initial value of the gravitational potential remains. This produces an *enhancement* in the transfer function as compared to the Maxwell-Boltzmann and Fermi-Dirac cases, in which the memory in the kernel is of much shorter range and the initial (maximum) value of the gravitational potential does not contribute as much to the integrand for $u \sim 1$.

This remarkable difference will be studied explicitly below in a comparison between the three cases.

For bosons eqs.(2.73) and (4.16) yield,

$$\alpha = \sqrt{\frac{\zeta(3)}{4 \zeta(5)}} \gamma = 0.538 \dots \gamma , \quad (4.22)$$

and we now have all the ingredients to study the transfer function as a function of γ to compare to the previous cases.

The analysis presented in the previous cases for the magnitude of the contributions from the Born and second (and higher) order remains the same. In the long wavelength limit $\gamma \ll 1$ the Born term dominates, and the second order correction is subleading of order $\mathcal{O}(\gamma^4)$.

For large γ (small scales) just as in the Maxwell-Boltzmann and Fermi-Dirac statistics, and quite generally, for $u \sim 0$ the integral of the kernel yields a contribution $\sim \gamma^4 u^4$, therefore for large γ the second order contribution begins to be significant at $u \sim 1/\gamma$ but at this time the gravitational potential has decayed significantly for $\gamma \gg 1$. Although the long range memory of the kernel maintains information on the initial values of the gravitational potential, but suppressed by a power $1/\gamma$. Therefore the second order correction becomes significant for large γ (small scales) but is also suppressed by inverse powers of γ , and hence is always perturbatively small.

It must be noticed that because of its longer range, the second order correction for bosons is comparatively *larger* to that in the Maxwell-Boltzmann and Fermi-Dirac case.

We have studied numerically the transfer function for both initial conditions and compared the exact numerical solution of Gilbert's equation to the Born term and the second order correction. Both cases are qualitatively similar. Fig. 9 displays the results of the analysis in the case of the initial conditions corresponding to temperature perturbations eq.(4.18). The results for Gilbert's initial conditions eq.(4.19) are qualitatively the same, with a remarkable agreement between the exact numerical solution and the second order improved Born approximation.

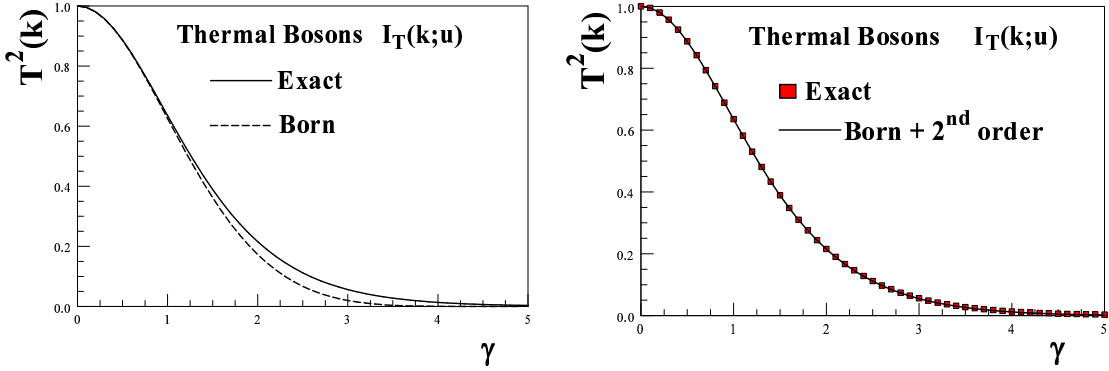


FIG. 9: Bosonic thermal relics. Left panel: $T^2(k)$ vs γ for the exact solution and the Born approximation. Right panel: $T^2(k)$ vs. γ for the exact solution and the Born approximation plus second order. Initial condition given by eq.(4.18) corresponding to temperature perturbations.

$T(k)$ for large scales follows from eq.(2.69) and

$$I_G[\alpha u] \stackrel{\alpha u \rightarrow 0}{\simeq} 1 - 2 \frac{\zeta(5)}{\zeta(3)} (\alpha u)^2 + \mathcal{O}([\alpha u]^4) ,$$

for bosons. We find that the large scale expression for $T(k)$ eq.(3.20) is **also valid** in the BE case.

The numerical solution of eq.(3.6) for bosons shows that $T(k)$ both for temperature and for Gilbert initial conditions [eqs.(2.65) and (2.66)] decreases as a power for $\gamma > 6$:

$$T(k) \simeq \left(\frac{\gamma_B}{\gamma} \right)^{x_B} , \quad x_B \simeq 4.8, \gamma_B \simeq 2.9 \text{ for temperature initial conditions ,}$$

$$x_B \simeq 4.6, \gamma_B \simeq 3.2 \text{ for Gilbert initial conditions .} \quad (4.23)$$

Again the scale of suppression of $T(k)$ **increases** with increasing k , from $\gamma_0 \simeq 1.62 \dots$ for small k to $\gamma_B \simeq 2.9 - 3.2$ for $\gamma > 6$. However, these scales are all of the same order $\sim \mathcal{O}(1)$, evidence of a *unique characteristic scale* $\gamma_{char} \sim \mathcal{O}(1)$. Namely, just as in the previous cases, in terms of the wavevector k the relevant scale of suppression is $k_{fs}(t_{eq})$.

V. SMALL SCALES: STATISTICS AND MEMORY OF GRAVITATIONAL CLUSTERING

The difference in statistics, namely the distribution function of the decoupled particles, enters in the initial condition and in the non-local kernel of Gilbert's equation (2.47). The initial conditions are determined from the evolution of

perturbations during the cosmological stages prior to matter domination and their dependence on the distribution function may be different from the ones studied in the previous sections, while the kernel in eq.(2.47) is independent of the initial conditions.

The study above revealed a remarkable difference arising from the different distribution functions. We have established that the free streaming solution described by $I[\alpha u]$ has very different asymptotics, falling off exponentially with αu in the case of Maxwell-Boltzmann and as power laws in the Fermi-Dirac and Bose-Einstein cases. Furthermore, the fall-off is much faster for fermions than for bosons. Since the maximum value of u is $u = 1$ the asymptotic behavior in γu actually describes the region $\gamma \gg 1$ or scales much smaller than the free streaming scale.

We have also highlighted that the different statistics lead to an important difference in the contributions from the kernel $K(u - u')$: whereas Maxwell-Boltzmann statistics leads to a short range memory that falls off exponentially in $(u - u')$ eq.(3.8), both Fermi-Dirac and Bose-Einstein lead to long-range memory that falls off with a power law in $(u - u')$ [eqs.(4.11) and (4.21)], the smallest power, namely the slowest fall-off corresponds to Bose-Einstein statistics as a consequence of the infrared enhancement (large population at small momentum).

Furthermore, we have shown in the previous sections that the influence of the kernel $K(u - u')$ (the second order correction) becomes important at small scales ($\gamma > 1$). The long-range of the kernel keeps memory of the early stages of the evolution when the gravitational perturbation has its largest amplitude, therefore the long-range nature of the kernel leads to an *enhancement* of the transfer function and the power spectrum at small scales as depicted in fig. 10.

We can study the small scale behavior in more detail by focusing on the time scales during which the gravitational potential varies slowly and a Markovian approximation, such as that discussed in section III A is reliable. As discussed above and explicitly shown by the numerical study, for $\gamma \gg 1$ the gravitational potential decays very rapidly over a time scale $u \sim 1/\gamma$, then after evolves slowly until $u \sim 1$. In order to gain deeper understanding of the dynamics during this time scale it is convenient to implement a Markovian approximation directly in Gilbert's equation (2.47). Upon changing variables in the integrand in eq.(2.47) $\alpha(u - u') \equiv z$, eq.(2.47) becomes

$$\Phi(k, u) - \frac{6}{\alpha^2} (1 - u)^2 \int_0^{\alpha u} \Pi[z] \frac{\Phi(k, u - \frac{z}{\alpha})}{[1 - (u - \frac{z}{\alpha})]^4} dz = (1 - u)^2 I[\alpha u], \quad (5.1)$$

where the kernel $\Pi[z]$ is given by eq.(2.41).

For the Maxwell-Boltzmann case [see eq.(3.6)] it is more convenient to change variables to $\gamma(u - u') \equiv z$.

The kernel $\Pi[z]$ vanishes at $z = 0$, is sharply peaked near $z \sim 1$ and falls off exponentially for Maxwell-Boltzmann (see eq.(3.6)), as $1/z^3$ for Fermi-Dirac and as $1/z$ for Bose-Einstein.

For $u \gg 1/\alpha$ and $(1 - u) \gg 1/\alpha$ the terms that multiply $\Pi[z]$ may be expanded in a power series expansion in z/α . This is the Markovian approximation, in which we obtain

$$\Phi(k, u) \Gamma[k; u] + \frac{6}{\alpha^3} (1 - u)^2 \frac{d}{du} \left[\frac{\Phi(k, u)}{(1 - u)^4} \right] \int_0^{\alpha u} \Pi[z] z dz \left[1 + \mathcal{O}\left(\frac{z^2}{\alpha^2}\right) \right] = (1 - u)^2 I[\alpha u]. \quad (5.2)$$

The first order equation (5.2) has a simple exponential solution that determines the decaying behavior of the gravitational perturbation, where the effective decay rate of gravitational perturbations $\Gamma[k; u]$ is given by

$$\Gamma[k; u] = 1 - \frac{6}{\alpha^2 (1 - u)^2} \int_0^{\alpha u} \Pi[z] dz \equiv 1 - \frac{K_{\Phi}^2(t)}{k^2}. \quad (5.3)$$

The wave-vectors leading to the smaller positive values of the decay rate Γ are the ones that decay the least and for which the power is the largest. This is akin to the criterion that determines the Jeans wave vector in a fluid with gravitational perturbations: the Jeans wave vector separates the stable acoustic oscillations from the unstable, growing modes corresponding to gravitational collapse. This is also the criterion that determines the free streaming wave-vector in Minkowski space-time [37].

For Maxwell-Boltzmann and Fermi-Dirac distribution functions the upper limit in the integrals can be safely taken to infinity for $\alpha u \gg 1$, with the result

$$\int_0^{\infty} \Pi[z] dz = \int_0^{\infty} \tilde{f}_0(y) dy = \left\langle \frac{1}{y^2} \right\rangle \quad (5.4)$$

$$\int_0^{\infty} z \Pi[z] dz = \mathcal{A}. \quad (5.5)$$

where the (finite) constant \mathcal{A} depends on the distribution function and the angular brackets stand for the average with \tilde{f}_0 . In these cases we find for $K_\Phi^2(t)$ [see eqs.(2.15) and (2.36)]

$$K_\Phi^2(t) = \frac{3}{2} H_{0M}^2 \frac{a_{eq}}{(1-u)^2} \left(\frac{m}{T_{d,0}} \right)^2 \left\langle \frac{1}{y^2} \right\rangle = 4\pi G \rho_{0M} \left\langle \frac{1}{\vec{V}^2} \right\rangle a(t) = K_\Phi^2(0) a(t). \quad (5.6)$$

Remarkably, $K_\Phi(t)$ coincides with the free streaming wave-vector found in Minkowski space-time [37],

$$K_\Phi(0) = \left[4\pi G \rho_{0M} \left\langle \frac{1}{\vec{V}^2} \right\rangle \right]^{\frac{1}{2}} = 0.563 \left[\left\langle \frac{1}{y^2} \right\rangle \right]^{\frac{1}{2}} \left(\frac{g_d}{2} \right)^{\frac{1}{3}} \frac{m}{\text{keV}} [\text{kpc}]^{-1}. \quad (5.7)$$

Thus, at small scales the Minkowski result is obtained, consistently with the expectation that at short wavelengths an adiabatic approximation to the expansion is reliable [32, 37].

The full transfer function $T(k)$ cannot be obtained from the Markovian approximation alone and the full study presented in the previous sections is necessary. However, it becomes clear that $k_{fs}(t_{eq})$ is not the *only* relevant scale and that there is a further scale $K_\Phi(t_{eq})$ eq.(5.7). The ratio of these two expressions is

$$\frac{K_\Phi^2(0)}{k_{fs}^2(0)} = \langle \vec{V}^2 \rangle \left\langle \frac{1}{\vec{V}^2} \right\rangle = \int_0^\infty y^4 \tilde{f}_0(y) dy \int_0^\infty \tilde{f}_0(y) dy = \begin{cases} 3 & \text{Maxwell - Boltzmann} \\ 4.9742\dots & \text{Fermi - Dirac} \end{cases}. \quad (5.8)$$

Defining the small scale length *today*

$$\Lambda_\Phi(t_{eq}) = \frac{2\pi}{K_\Phi(t_{eq})} \quad (5.9)$$

we find for WIMPs,

$$\Lambda_\Phi(t_{eq}) \sim 0.5 \text{ pc} \left(\frac{2}{g_d} \right)^{\frac{1}{3}} \left(\frac{100 \text{ GeV}}{m} \right)^{\frac{1}{2}} \left(\frac{10 \text{ MeV}}{T_d} \right)^{\frac{1}{2}}, \quad (5.10)$$

and for thermal fermions,

$$\Lambda_\Phi(t_{eq}) = 939 \text{ kpc} \left(\frac{2}{g_d} \right)^{\frac{1}{3}} \frac{\text{keV}}{m} \quad \text{FD} \quad . \quad (5.11)$$

The results above are valid for both Maxwell-Boltzmann and Fermi-Dirac statistics, in these cases the kernel $\Pi[z]$ falls off fast enough to make its integral finite. This is *not* the case for Bose-Einstein statistics for particles that decoupled in LTE while ultrarelativistic. In this case the asymptotic behavior of $\Pi[z] \propto 1/z$ leads to an *infrared* enhancement as a consequence of the long-range of the kernel. In this case we keep the upper limit in eq.(5.3) and carry out the integral in z , leading to [50]

$$\int_0^{\gamma u} \Pi[z] dz = \frac{1}{2\zeta(3)} \int_0^\infty \frac{dy}{e^y - 1} [1 - \cos(\gamma u y)] \stackrel{\gamma u \rightarrow \infty}{=} \frac{\ln[\gamma u e^{\mathcal{C}}]}{2\zeta(3)}. \quad (5.12)$$

where $\mathcal{C} = 0.577216\dots$ is the Euler-Mascheroni constant as well as in the coefficient of the derivative term in eq.(5.2), leading to

$$\int_0^{\gamma u} z \Pi[z] dz \stackrel{\gamma u \rightarrow \infty}{=} \frac{\gamma u}{2\zeta(3)}. \quad (5.13)$$

This infrared enhancement reflects the infrared divergence of the free streaming wavevector in Minkowski space-time found in ref.[37]. The argument of the logarithm in eq.(5.12) clearly reveals that it is the cosmological expansion that yields an infrared cutoff. Taking $u \sim 1$ [neglecting terms of $\mathcal{O}(1/\gamma)$] we find a sliding wavevector at small scales for the Bose-Einstein case, namely

$$K_\Phi(t_{eq}) \simeq 0.00424\dots \sqrt{\ln \gamma + \mathcal{C}} \left(\frac{g_d}{2} \right)^{\frac{1}{3}} \frac{m}{\text{keV}} [\text{kpc}]^{-1} \quad \text{BE} \quad . \quad (5.14)$$

The larger $K_\Phi(t_{eq})$ leads to shorter free streaming lengths and to more power at small scales because free streaming smoothes out on shorter scales. Therefore, at *small scales* BE particles that decoupled while relativistic behave as

CDM. This conclusion is in agreement with the results in refs. [37, 39] and is borne out in the numerical solution displayed in fig. (10).

In all cases $K_{\Phi}(t_{eq})$ controls the decay of the gravitational fluctuations $\Phi(k, u)$ for small scales and long times. The logarithmic behavior and the consequent increase of K_{Φ} yields an explanation of the enhancement at small scales over the FD and MB cases depicted in fig. (10).

Comparing statistics and initial conditions:

The analysis presented above clearly indicates the differences arising from statistics and initial conditions. It proves convenient to compare the results of the numerical solution of Gilbert's equations for all cases considered parametrized by the dimensionless ratio γ . This comparison is depicted in fig. 10 for a wide range of γ . The differences from statistics and initial conditions are clearly displayed in this figure, and are in complete agreement with the analysis presented above.

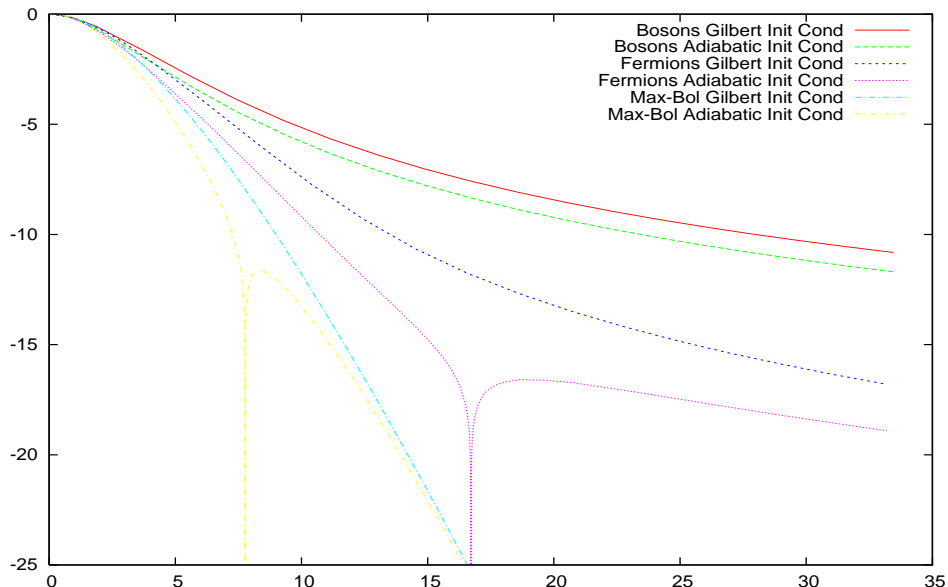


FIG. 10: Comparison of exact numerical solutions of eq.(2.47) and (2.61) for $\ln|T(k)|$ vs. γ for Maxwell-Boltzmann particles, fermion and boson thermal relics with Gilbert and temperature initial conditions eqs.(2.65) and (2.66).

For thermal relics that decoupled while relativistic, either FD or BE, the range of scales relevant for structure formation in which the linearized approximation is reliable corresponds to $0 < \gamma \leq 6$, whereas for WIMPs, the relevant range of scales corresponds to $\gamma \leq 10^{-5}$. We have confirmed that in the range of cosmological relevance for all species, the second order approximation (2.111) for $T(k)$ is *very accurate* and indistinguishable from the exact numerical solution in the range $0 < \gamma \leq 6$.

As shown in fig. 10 $T(k)$ features zeroes for MB and FD statistics for temperature initial conditions. However the value of γ for FD at which $T(k)$ vanishes corresponds to a sub-galactic scale, and for MB it corresponds to a sub-parsec scale, in either case well outside the regime of reliability of the linearized approximation, hence these features are not relevant for structure formation. Nevertheless, this figure highlights the main aspects discussed above: for a *fixed* value of γ BE statistics favors the small momentum region, leads to a longer range memory kernel that falls off with a power law and yields the largest $T(k)$ for a fixed value of γ , followed by FD statistics with a (slower) power law fall off and finally the MB distribution with an exponential fall off of the memory kernel and the smallest $T(k)$ for fixed γ .

VI. CONCLUSIONS

In this article we studied the evolution of gravitational and DM density perturbations from the collisionless Boltzmann-Vlasov during matter domination, and obtained an *exact* expression for the transfer function $T(k)$ for *arbitrary distribution function of the decoupled DM particle and initial conditions*.

We have transformed the non-relativistic Boltzmann-Vlasov equation into an integro-differential equation which features a non-local kernel that describes the memory of gravitational clustering and yields corrections to the fluid

description. This formulation lends itself to a systematic Fredholm expansion for the evolution of DM density and gravitational perturbations and $T(k)$, and makes explicit the influence of the distribution function on $T(k)$.

Distribution functions that favor the small momentum region lead to *longer range* kernels, a persistence of the memory of the initial conditions and gravitational clustering resulting in an *enhancement* of $T(k)$ at *small scales*.

The natural scale of suppression of $T(k)$ is determined by the free-streaming wave vector at matter-radiation equality, $k_{fs}(t_{eq}) = \sqrt{6}/l_{fs}(0)$ where the comoving free streaming wavevector is

$$k_{fs}(t) = \left[\frac{4\pi\rho_{0M}a(t)}{\langle \left(\frac{\vec{p}}{m}\right)^2 \rangle} \right]^{\frac{1}{2}}, \quad (6.1)$$

the angular brackets refer to the average with the distribution function of the decoupled particle, and $l_{fs}(0)$ is the comoving free streaming distance traveled by the decoupled particle from the time of matter-radiation equality t_{eq} until today.

We find

$$k_{fs}(t_{eq}) = \frac{k_{fs}(0)}{\sqrt{1+z_{eq}}} \quad (6.2)$$

with

$$k_{fs}(0) = \begin{cases} \frac{0.325}{[10^{-3}\text{pc}]} \left(\frac{g_d}{2}\right)^{\frac{1}{3}} \left(\frac{m}{100\text{GeV}}\right)^{\frac{1}{2}} \left(\frac{T_d}{10\text{MeV}}\right)^{\frac{1}{2}} & \text{WIMPs} \\ 0.157 \left(\frac{g_d}{2}\right)^{\frac{1}{3}} \left(\frac{m}{\text{keV}}\right) [\text{kpc}]^{-1} & \text{FD thermal relic} \\ 0.175 \left(\frac{g_d}{2}\right)^{\frac{1}{3}} \left(\frac{m}{\text{keV}}\right) [\text{kpc}]^{-1} & \text{BE thermal relic} \end{cases} \quad (6.3)$$

where g_d is the number of relativistic species at decoupling.

We provided a detailed numerical study for thermal relics, WIMPs and fermionic and bosonic particles that decoupled while relativistically. The result of the numerical study of $T(k)$ as a function of $\gamma = \sqrt{2}k/k_{fs}(t_{eq})$ for the three cases and different initial conditions is displayed in fig. 10.

This study reveals that the first *two* terms in the Fredholm expansion yield a remarkable accurate approximation to $T(k)$ in the range of scales of cosmological relevance for structure formation. In all cases considered we find that the exact solution differs from the second order approximation in less than 5% in the range $0 < \gamma \lesssim 6$ corresponding to scales down to a fraction of the free-streaming length and much less than this on large scales for $0 < \gamma \lesssim 1$.

A simple and accurate approximation to $T(k)$ is given by eqn. (2.111). The second term in this expression includes corrections beyond the fluid approximation and higher order moments in the Boltzmann hierarchy and describes the memory of initial conditions and gravitational clustering. It explicitly depends on the distribution function of the decoupled particle. Non-local kernels with longer range lead to an *enhancement* of $T(k)$ at small scales. FD and BE thermal relics feature kernels with longer range than WIMPs, with BE statistics (for relics that decoupled relativistically) leading to longer range and more power at small scales.

This behavior is clearly exhibited in fig. 10.

For long scales $k \ll k_{fs}(t_{eq})$ we find the behavior

$$T(k) = 1 - \left(\frac{\gamma}{\gamma_0}\right)^2 + \dots \quad (6.4)$$

where γ_0 is given by (3.21) for the initial conditions considered here independent of the statistics for thermal relics.

We provide fits of $T(k)$, within a wide range of (small) scales for $k > k_{fs}(t_{eq})$ in the intervals where it exhibits a simple power-like or exponential behavior for MB, FD and BE statistics: see eqs.(3.22), (4.13), (4.14), (4.15) and (4.23).

Although we do not attempt to provide a global fit with *one* function, it is clear that in the small scale region, the functional forms of $T(k)$ found in this article by exact numerical solution of the Boltzmann-Vlasov equation (in Gilbert's form) are very different from the fits by Bardeen *et.al.*[51] often quoted in the literature.

An important consequence of this study is a distinct imprint of the particle statistics and its distribution function on the transfer function at *small scales*, $\lambda \ll l_{fs}(0)$: a distribution function that enhances the *small* momentum

region yields a *longer range memory* of the initial conditions and gravitational clustering and an *enhancement* of the transfer function at small scales as depicted in fig. 10. This result may prove important in the elucidation of the small scale structure of DM halos and perhaps lead to an explanation of the filamentary structures found in numerical simulations in ref.[52].

The tools provided in this article to study the transfer function for arbitrary distribution functions and general initial conditions, in particular the simple and remarkably accurate approximation to $T(k)$ given by eqn. (2.111) allows a systematic and robust assessment of different DM candidates.

Acknowledgments

D.B. thanks Andrew Zentner and Alex Kusenko for stimulating discussions and insight. He acknowledges support from the U.S. National Science Foundation through grant No: PHY-0553418.

-
- [1] S. Dodelson *Modern Cosmology*, Academic Press, N.Y. 2003.
 - [2] E. W. Kolb, M. S. Turner, *The Early Universe*, Addison-Wesley, Redwood City, CA, (1990).
 - [3] B. Moore *et. al.*, *Astrophys. J. Lett.* **524**, L19 (1999).
 - [4] G. Kauffman, S. D. M. White, B. Guiderdoni, *Mon. Not. Roy. Astron. Soc.* **264**, 201 (1993).
 - [5] S. Ghigna *et.al.* *Astrophys.J.* **544**,616 (2000).
 - [6] A. Klypin *et. al.* *Astrophys. J.* **523**, 32 (1999); *Astrophys. J.* **522**, 82 (1999).
 - [7] B. Willman *et.al.* *Mon. Not. Roy. Astron. Soc.* **353**, 639 (2004).
 - [8] J. F. Navarro, C. S. Frenk, S. White, *Mon. Not. R. Astron. Soc.* **462**, 563 (1996).
 - [9] J. Dubinski, R. Carlberg, *Astrophys.J.* **378**, 496 (1991).
 - [10] J. S. Bullock *et.al.*, *Mon.Not.Roy.Astron.Soc.* **321**, 559 (2001); A. R. Zentner, J. S. Bullock, *Phys. Rev.* **D66**, 043003 (2002); *Astrophys. J.* **598**, 49 (2003).
 - [11] J. Diemand *et.al.* *Mon.Not.Roy.Astron.Soc.* **364**, 665 (2005).
 - [12] J. J. Dalcanton, C. J. Hogan, *Astrophys. J.* **561**, 35 (2001).
 - [13] F. C. van den Bosch, R. A. Swaters, *Mon. Not. Roy. Astron. Soc.* **325**, 1017 (2001).
 - [14] R. A. Swaters, *et.al.*, *Astrophys. J.* **583**, 732 (2003).
 - [15] R. F. G. Wyse and G. Gilmore, arXiv:0708.1492; G. Gilmore *et. al.* astro-ph/0703308; G. Gilmore *et.al.* arXiv:0804.1919; G. Gilmore, astro-ph/0703370.
 - [16] G. Gentile *et.al.* *Astrophys. J. Lett.* **634**, L145 (2005); G. Gentile *et.al.*, *Mon. Not. Roy. Astron. Soc.* **351**, 903 (2004); V. G. J. De Blok *et.al.* *Mon. Not. Roy. Astron. Soc.* **340**, 657 (2003), G. Gentile *et.al.*, astro-ph/0701550; P. Salucci, A. Sinibaldi, *Astron. Astrophys.* **323**, 1 (1997).
 - [17] G. Battaglia *et.al.* arXiv:0802.4220.
 - [18] M. Ryan Joung, R. Cen, G. L. Bryan, arXiv:0805.3150.
 - [19] R. Wojtak *et.al.* arXiv:0802.0429.
 - [20] B. Moore, *et.al.* *Mon. Not. Roy. Astron. Soc.* **310**, 1147 (1999);
 - [21] P. Bode, J. P. Ostriker, N. Turok, *Astrophys. J* **556**, 93 (2001)
 - [22] V. Avila-Reese *et.al.* *Astrophys. J.* **559**, 516 (2001).
 - [23] J. R. Bond, A. S. Szalay, *Astrophys. J.* **274**, 443 (1983).
 - [24] P. J. E. Peebles, *The Large-Scale Structure of the Universe*, Princeton Series in Physics, Princeton University Press, Princeton, N.J. 1980.
 - [25] E. Bertschinger, in *Cosmology and Large Scale Structure*, proceedings, Les Houches Summer School, Session LX, ed. R. Shaeffer *et. al.* (Elsevier, Amsterdam), 273 (1996).
 - [26] N. A. Krall, A. W. Trivelpiece, *Principles of Plasma Physics*, San Francisco Press, Inc. San Francisco, CA (1986); S. Ichimaru, *Statistical Plasma Physics, volume 1: Basic Principles*, Westview Press, Boulder, Colorado, 2004; R. D. Hazeltine, F. L. Waelbroeck, *The Framework of Plasma Physics*, Westview Press, Boulder, Colorado, 2004).
 - [27] J. Binney, S. Tremaine, *Galactic Dynamics*, Princeton University Press, Princeton, New Jersey, (1987); W. Saslaw *Gravitational Physics of Stellar and Galactic Systems*, Cambridge University Press, Cambridge, UK, (1985); G. Bertin, *Dynamics of Galaxies*, Cambridge University Press, Cambridge, UK, (2000).
 - [28] R. W. Nelson, S. Tremaine, *MNRAS* **306**, 1 (1999).
 - [29] I. H. Gilbert, *Astrophys. J.* **144**, 233 (1966); *ibid*, **152**, 1043 (1968).
 - [30] R. Brandenberger, N. Kaiser, N. Turok, *Phys. Rev.* **D36**, 2242 (1987).
 - [31] E. Bertschinger, P. N. Watts, *Astrophys. J.* **328**, 23 (1988).
 - [32] A. Ringwald, Y. Y. Y. Wong, *JCAP* **0412**, 005 (2004).
 - [33] A. Palazzo *et.al.*, arXiv:0707.1495.
 - [34] S. Dodelson, L. M. Widrow, *Phys. Rev. Lett.* **72**, 17 (1994).

- [35] X. Shi, G. M. Fuller, Phys. Rev. Lett. **82**, 2832 (1999); K. Abazajian, G. M. Fuller, M. Patel, Phys. Rev. **D64**, 023501 (2001); K. Abazajian, G. M. Fuller, Phys. Rev. **D66**, 023526, (2002); G. M. Fuller *et. al.*, Phys.Rev. **D68**, 103002 (2003); K. Abazajian, Phys. Rev. **D73**,063506 (2006); M. Shaposhnikov, I. Tkachev, Phys. Lett. **B639**,414 (2006).
- [36] A. Kusenko, hep-ph/0703116; astro-ph/0608096; T. Asaka, M. Shaposhnikov, A. Kusenko; Phys.Lett. **B638**, 401 (2006); P. L. Biermann, A. Kusenko, Phys. Rev. Lett. **96**, 091301 (2006).
- [37] D. Boyanovsky, Phys. Rev. **D 77**, 023528 (2008).
- [38] C. J. Hogan, J. J. Dalcanton, Phys. Rev. **D62**, 063511 (2000).
- [39] D. Boyanovsky, H. J. de Vega, N. Sanchez, Phys. Rev. **D 77**, 043518 (2008).
- [40] K. Petraki, A. Kusenko, Phys. Rev. **D 77**, 065014 (2008); K. Petraki, Phys. Rev. **D 77**, 105004 (2008); M. Laine, M. Shaposhnikov, JCAP 0806 (2008) 031.
- [41] S. Tremaine, J. E. Gunn, Phys. Rev. Lett. **42**, 407 (1979); D. Lynden-Bell, Mon. Not. Roy. Astron. Soc. **136**, 101 (1967), S. Tremaine, M. Henon, D. Lynden-Bell, Mon. Not. Roy. Astron. Soc. **219**, 285 (1986).
- [42] U. Seljak, M. Zaldarriaga, Astrophys. J. **469**, 437 (1996); W. Hu. U. Seljak, M. White, M. Zaldarriaga, Phys. Rev. **D57**, 3290 (1998).
- [43] A. Lewis, A. Challinor, A. Lasenby, Astrophys. J. **538**, 473 (2000).
- [44] C.-P. Ma, E. Bertschinger, Astrophys. J. **455**, 7 (1995).
- [45] D. J. Eisenstein, W. Hu, Astrophys. J. **496**, 605 (1998).
- [46] W. Hu, N. Sugiyama, Astrophys. J. **471**, 542 (1996).
- [47] D. J. Eisenstein *et.al.* Astrophys. J. **633**, 560 (2005).
- [48] A. M. Green, S. Hofmann, D. J. Schwarz, JCAP **0508** 003 (2005); S. Hofmann, D. Schwarz, H. Stocker, Phys. Rev. **D64**, 083507 (2001); A. M. Green, S. Hofmann, D. J. Schwarz, Mon. Not. Roy. Astron. Soc. **353** L23 (2004); T. Bringmann, S. Hofmann, JCAP **0407**, 016 (2007), and references therein.
- [49] P. M. Morse, H. Feshbach, *Methods of Theoretical Physics*, McGraw-Hill, New York, 1953.
- [50] D. Boyanovsky, H. J. de Vega, Ann. Phys. **307**, 335 (2003).
- [51] J M Bardeen et al. Astrophys. J. **304**, 15 (1986).
- [52] L. Gao, T. Theuns, Science, **317**, 1527, (2007).